Regional Studies in Marine Science
March 2022, Volume 51, Pages 102219 (15p.)
https://doi.org/10.1016/j.rsma.2022.102219
https://archimer.ifremer.fr/doc/00751/86263/

T-S and hydrodynamical structures within the deltaic regions and continental platforms adjacent to two northeastern Brazilian rivers

Capuano Tonia Astrid [1, *], Araujo Moacyr [1], Silva Marcus [1], Varona Humberto L. [1], Cambon Gildas [2], Koch-Larrouy Ariane [3]

[1] Laboratorio de Oceanografia Física, Estuarina, e Costeira (LOFEC), Departamento de Oceanografia da Universidade Federal de Pernambuco (UFPE), Recife, Brazil
[2] Laboratoire d' Océanographie Physique et Spatiale (LOPS), IUEM, Univ. Brest, CNRS, IRD, Ifremer, Brest, France
[3] Laboratoire d'Etudes en Géophysique et Océanographie Spatiales (LEGOS), 18 avenue Edouard Belin, 31401, Toulouse Cedex 9, France

* Corresponding author : Tonia Astrid Capuano, email address : toniacapuano@yahoo.it

Abstract :

The delta-front estuaries of large rivers are crucial interfaces between lands and oceans, being considered hotspots of vulnerability to the impact of climate changes due to several causes: sea level rise; changes in the river discharges driven by climatic alterations in the hydrographic basins; high human concentration and other anthropic factors. This study focuses on the hydrodynamics/circulation and T-S structure within the shelf regions and continental platform adjacent to two among the major rivers of Northeastern Brazil: the Sao Francisco and Parnaiba. We aim to qualitatively and quantitatively describe the physical dynamics typical of these coastal regions and try to relate their main alterations to the effects of local mechanisms as tidal forcing. The choice of these deltas was motivated by the great potential that such, biodiverse regions have in acting as important proxies of environmental modifications affecting the Brazilian tropical zone, allowing to investigate the role of geographical variability in response to these changes. A series of regional, modelling simulations was realized, at increasingly higher resolutions, in order to assess the mean and seasonal spatio-temporal variability of physical properties (T-S distribution, salt transport, hydrodynamical features of the local circulation). The identification and analysis of the major scales of variability was also used to evaluate the performance and applicability of our numerical tool, the Regional Ocean Modelling System, in the study areas. Preliminary results on mesoscales processes indicate that both deltas are modulated by an intense turbulent activity. The continental platform near the Sao Francisco estuary is marked by the presence of subsurface-intensified vortices, and the one in proximity of the Parnaiba mouth is characterised by the appearance of small vortices, fine meanders and filaments probably triggered by non-linear interactions between the river plume and the North Brazilian Current rings.

Keywords : Rivers' deltas, T-S properties, mesoscale eddies, Tropical Atlantic, ROMS.

SECTION 1: INTRODUCTION

Large-river, delta-front estuaries are important interfaces between continents and the oceans for material fluxes that have a global impact on the coastal dynamics and marine biogeochemistry. Changes in the climate system of the last millenniums seemed to have caused alterations in the hydrographic basins of the major rivers of our planet, affecting the sediments discharges in their estuaries, as already demonstrated by several authors for different regions of the world ocean [*Yang et al., 2002; Xu, 2003; Donner et al., 2004; Kundzewicz Z. W. et al., 2008; Bianchi and Allison, 2009; Araujo et al., 2014, 2017*]. Because long-term preservation of high-resolution sedimentary records on eroding continental platforms is rare, and where present, often integrates conditions from only a limited region, we must rely on coastal marine sediments (especially in large river deltas from estuaries) to better advance our understanding of continental climatic processes. Hence, the deltaic clinoforms built by these huge rivers represent an important source of underestimated informations on environmental changes. This results from the fact that these deltaic regions are mainly characterized by an elevated rate of sediments and nutrients deposition allowing the preservation of different types of environmental proxies, in opposition to what happens in areas located far from the river mouth where the sediments transport is more easily eroded, producing incomplete, environmental records.

In our study, we will particularly focus on the deltas and adjacent continental platforms of two among the major rivers of Brazil, located in the Northeastern corner of the country: the Sao Francisco and the Parnaiba (Figure 1). The choice of these estuarine environments was motivated by the great potential that they have in acting as important proxies of the environmental modifications (sea level rise, alterations in the river discharges, etc.) affecting the tropical zone of Brazil, allowing to investigate the role of geographical variability in response to local to regional changes. With this aim, we have realized a series of realistic, modelling simulations in order to qualify and quantify the mean and seasonal spatio-temporal variability of physical properties: thermo-haline structure, river discharge, main hydrodynamical features of the regional circulation.

We will numerically explore the complex dynamics of these two deltaic systems in order to investigate alterations in the spatio-temporal distribution of the key physical processes of the study areas in relation to short-term environmental factors. For this purpose, our present work builds upon past numerical and observational findings [*Silva A. C. et al., 2005, 2009b, 2010; Silva M. et al., 2009a; Landim Dominguez et al., 2012; Araujo et al.,*

2014, 2017 2018; Varona et al., 2019]. Some were used to gather together all the available information collected in precedent in-situ campaigns, but also to take advantage of the modelling work started at the Federal University of Pernambuco simulating the hydrodynamical circulation of the Western Tropical Atlantic.

The paper is organized as follows. The current Sect. 1 ends up with a brief presentation of the oceanographic region of study. The main aspects of the numerical model used for our experiments and details about its configurations are introduced in Sect. 2, as well as the satellite products employed for the comparison of its output with observations. In this section we also provide a description of the salt transport calculation with its physical meaning, hydrodynamical implications and the specific applications of this estimate made in our work. In Sect. 3, our principle modelling results in terms of thermo-haline structure and mesoscale processes, are presented in order to highlight the strong variability and high, dynamical complexity of the estuarine-coastal areas under investigation. In section 4, we discuss the principal results obtained from our numerical simulations relating them with previous findings, documented in literature, and conclude with some final remarks and perspectives on future steps to improve our work.

The ocean circulation along the Northeastern Brazilian coast (Figure 1b) performs an important role in the interhemispheric transport of mass, heat, and salt and in the thermo-haline overturning cell of the Western Tropical North-Atlantic Ocean (WTNA) [*Schmitz Jr. and McCartney, 1993; Bourlès et al., 1999a; Silva et al., 2009a; Veleda et al., 2012*]. The WTNA is characterised by a complex system of zonal currents and counter-currents forced by subtropical gyres and the action of the trade winds in both hemispheres [*Stramma et al., 2005*]. The WTNA is also a region with an intense land-ocean interaction, marked by significant material transport, mixed-layer depth changes [*Grodsky et al., 2012; Coles et al., 2013]* and high biogeochemical activity [*Lefèvre et al., 2010; Ibánhez et al., 2017; Araujo et al., 2014, 2017]*, giving rise to alterations in local and remote oceanic processes. For example, rivers discharge uses to be a small component of the open ocean salinity balance, but the magnitude of the Amazon freshwater source is so important that the discharged volume reaches two-times the net evaporation minus precipitation (E-P) budget over the North-western Tropical Atlantic [*Ferry and Reverdin, 2004]*. Moreover, the estuaries of equatorial rivers have been identified as particularly high-energy marine systems because of the combined action of the currents in the western Atlantic Ocean, trade winds, tidal oscillations and the discharge of continental waters, from the Orinoco River and especially from the Amazon River *[Nittrouer and Demaster, 1996; Silva et al.,*

2010]. Thus, in addition to these physical and weather/climate mechanisms, other two major regional rivers, the Sao Francisco and the Parnaiba, are also responsible of providing relevant amounts of sediments, nutrients, and coloured as well as transparent dissolved organic matter that can be traced far from the rivers' mouths [*Hu et al., 2004*].

In particular, the Sao Francisco River (Figure 1d, displaying its deltaic region and the adjacent continental platform) is the fourth, major river of South-America. It constitutes the largest river to run entirely within Brazil, measuring a total of 2863 km and draining an area of 639,219 km^2, which represents 7.5% of Brazilian territory [*Knoppers et al., 2006*]. Along the Sao Francisco River estuary, the spring and neap tide have been observed to range from 1.8 to 0.8 m, respectively [Cavalcante et al., 2017]. The Sao Francisco is considered a classic example of a wave-dominated or wave-influenced delta [*Wright and Coleman, 1973; Bittencourt et al., 1982; Dominguez et al., 1987; Dominguez, 1996; Bhattacharya and Giosao, 2003; Rangel and Dominguez, 2015*], where high wave energy and mesotidal forcing induce intense vertical mixing of the estuarine zone and constant resuspension of particulates affect chemical processes [Bernardes et al., 2012]. This river plays an important role in the economy of the Northeastern region of Brazil, not only in terms of energy production but also as a source of water supply for the local population and agro-industrial activities developing within its basin. The Sao Francisco basin is considered one of the most vulnerable in Brazil to ongoing climate changes, suffering under a forecast of decreasing rainfall over the next decades [*Marengo et al., 2012*]. In its subaqueous portion, the Sao Francisco River has built a mud clinoform measuring about 30m in thickness [*Rangel, 2017*]. Delta clinoforms have long been recognized as natural records of environmental changes in the drainage basin and coastal sea [*Bianchi and Allison, 2009*]. This river has thus been in the last years object of an extensive, research effort [*Bittencourt et al., 2005; Marengo et al., 2012; Landim Dominguez et al., 2012; Araujo et al., 2014, 2018*] mainly aimed at evaluating the effects of huge dams on its hydro-sedimentologic regime and on the one of the adjacent coastal area, due to the sediments and nutrients' retention on the big reservoirs created by these dams. In most of these studies, the hydrological series of the 1930-1979 period has been used as a reference parameter for the analyses of changes and their environmental impact. After the 1979's flood, the reconstructed natural outflow of the Sao Francisco river has been characterised by an average discharge of 2.760 m^3/s and nowadays its mean values are even lower than this threshold [*Landim Dominguez et al., 2012].* The outflow reduction has been attributed to the construction and implementation of the above-mentioned dams,

starting from the Sobradinho one built in 1979. However, more recent studies [*Aquino da Silva et al., 2015; de Paula Filho et al., 2015*] suggest that this reduction in the outflow could also be related to a climatic signature, which could be responsible of up to 40% of this decrease. Indeed, the effects of the actual global warming could result in a general attenuation of the precipitations regime within the Sao Francisco basin and consequently in its outflow. Climate numerical models show that these effects could explain up to 35% of the reduction in precipitation within the hydrographic basin of the Sao Francisco River.

Similar considerations can be drawn for the Parnaiba River (Figure 1c), representing another important river of the Northeastern Brazilian coast, whose catchment area has a dendritic pattern covering ~344,112 km^2 and an average discharge of 841 m^3/s [*Aquino da Silva et al., 2015]*. The same authors report that in this region the tidal regime is semidiurnal and mesotidal, with a mean amplitude of about 1.70m at neap tide and an average 3.06m at spring tide. Apart from being characterized by a smaller length (~1400km) and a different dynamical regime, its region and the adjacent continental platform are submitted to a more limited, anthropic influence, in comparison to the Sao Francisco River, providing an interesting study area for the dynamical analysis of less contaminated, natural deltas. In fact, the Parnaiba mouth is an example of deltas presenting weak alterations in the transport of sediments. The investigation of the evolution and hydrodynamical regime of these deltas is therefore necessary at regional scales, in order to evaluate the effects of climate changes and sea level rise. This would precisely be the case of the Parnaiba River, where a small dam situated 630 km upstream of the mouth seems to not substantially affect the sediments transport towards the coast. This delta could be divided into two main areas: 1) an area laying between the two affluent tributaries of the Parnaiba River (the Parnaiba and the Igaraçu rivers), with their mouth oriented north-eastward; 2) a system of tidal channels further west, which extend in the nortwest-southeast direction [*Galloway, 1975; Bhattacharya and Giosao 2003*]. Faulting and the eastward inclination of the river mouth could be responsible of triggering a more recent transformation of the delta from the west to the east directions [*Almeida Filho et al., 2009]*. This could explain the erosive character and the ‘elbow’-shape of the principal channel of the river mouth within the upstream direction, which constitutes a typical characteristic of the tectonically-controlled, river outflows [*Reading and Collinson, 1996*].

In summary, deltas and their clinoforms are important repository of information about environmental changes (climate, variations in the sea level, anthropic impacts) affecting the rivers basins and the nearby coastal zones. Hence, our analysis of the major,

spatio-temporal scales of variability in the hydrodynamics and circulation of these deltaic regions and the adjacent continental platform would contribute to dynamically describe the coastal responses of these complex systems and elaborate predictions of responses to the effects of the ongoing climate changes. Moreover, the methodology developed in this paper could be extended and adapted to the oceanographic assessment of other understudied Brazilian rivers and to their adjacent oceanic regions.

SECTION 2: METHODOLOGY

The main goal of this work is to describe, through combining the analysis of satellite data and the output of numerical simulations, the main physical mechanisms determining the spatio-temporal distribution of the thermo-haline structure and the hydrodynamical regime/ circulation of the deltaic regions and the continental platform adjacent to the Sao Francisco and Parnaiba rivers. We actually aim to develop and obtain a reliable numerical tool, able to reproduce the different scales of variability of the T-S and mesoscale processes observed within the deltaic regions under study, in order to calibrate and validate our mathematical model: the Regional Ocean Modelling System (ROMS, *https://www.myroms.org/*).

The identification and analysis of the major scales of spatio- temporal variability of the thermo-haline and hydrodynamical variables, extracted from the numerical experiment for the deltaic regions under study, will be finally used to evaluate the performance and applicability of this model within the areas of interest.

2.1. ROMS MODEL

The numerical tool used for the above-mentioned objective, ROMS [*Shchepetkin and McWilliams, 2003, 2005; Penven et al., 2006; Debreu et al., 2012],* is a free-surface, terrain-following coordinate model with split-explicit time stepping and with Boussinesq and hydrostatic approximations. This model has been employed in many regions of the world ocean by a broad, international community. For our simulations we used the ROMS version developed at the 'Institut de Recherche pour le Développement' (IRD), where the ROMSTOOLS package [*Penven et al., 2006*] is available for creating the initial configurations and for the subsequent visualization and analysis of its output.

This ROMS version also allows the nesting of various grids ones into the others, thus increasing their individual resolutions, through the adoption of the AGRIF library

(Adaptative Grid Refinement in Fortran) [*Blayo and Debreu, 1999; Debreu, 2000; Debreu and Vouland, 2003; Debreu and Blayo, 2008*]. Two modes of communication are then possible between the different grids of a nested simulation: the 'one-way', also called 'downscaling', where the parent grid (at lower resolution) signals are used as boundary conditions for the child grid (at higher resolution, up to 3 times finer than the parent resolution, as in our work); 2) the 'two-way', where the signals of the child grid also feed back in to the parent grid, though a process known as 'upscaling'.

It is worth mentioning that ROMS has already been extensively tested in our oceanic area of interest and largely used by a team of Brazilian modellers placed at the Federal University of Pernambuco [*Silva A. C. et al., 2005, 2009b, 2010; Silva M. et al., 2009a; Varona et al., 2019].* Another remarkable advantage of this model is that has been designed to be run at regional scales, both within an idealised framework and in a realist context. It is indeed quite straightforward to realize sensitivity tests with this model by differently tuning a wide range of parameters, which enables the challenging pursuit of process-oriented studies. ROMS has also been designed for parallelization and computing optimization, so that our nested numerical experiments have been compiled using the MPI (Message Passing Interface) library. This numerical code has been satisfactorily implemented on the French supercomputing clusters of IDRIS, of which we used the latest machine named Jean-Zay (http://www.idris.fr/annonces/annonce-jean-zay.html).

As it regards the main datasets used to force and initialize our numerical experiments, at the lateral boundary and initial conditions all variables were constrained by the monthly mean of the 2009 World Ocean Atlas, WOA2009 [*Locarnini et al., 2010; Antonov et al., 2010]* with a resolution of 1°. The surface forcings were obtained from the monthly mean climatology of the Comprehensive Ocean-Atmosphere Data Set (COADS05) *[Da Silva et al., 1994]* with 0.5° of resolution. For the river discharge, we took advantage of the climatology of *Dai and Trenberth [2002],* which includes monthly means' values for the biggest South-American rivers' runoff. To verify if this dataset well reproduces the mean values of discharge for the two rivers under study, we have plotted a monthly time series for both the Sao Francisco and the Parnaiba (Supplementary Material 1) displaying a range of seasonal values well comparable to the ones reported in the regional literature (not shown). Tides are a key process in mixing the river freshwater plumes with the open ocean, and were obtained from the TPXO7 *[Egbert et al., 1994; Egbert and Erofeeva, 2002]*, encompassing altimetry data from several satellites in order

to validate the results obtained through the hydrodynamic model *[Wang, 2004; D'Onofrio et al., 2012]*. Hence, in our study we have tested the tidal effects on the local ocean dynamics, running a series of numerical simulations with and without the input of tides (respectively the "Tidal" and "No- tide" setups).

In particular, we primarily run these two configurations at a mesoscale-resolving, horizontal resolution of 1/12° (~7.3 km) using a geographical domain encompassing the whole Northeastern Brazilian coast: going from 10°N to 20°S of latitude and 30° to 60°W of longitude (Figure 1b). In this preparation phase, a reference configuration for the tidal components was developed. Additional numerical tests have been performed to check the sensitivity of the model solution to the vertical grid of the configuration (number of vertical levels, vertical resolution, value of the stretching parameters at the surface and bottom, etc.). By default ROMS tends to stretch the vertical levels towards the ocean surface, ensuring an enhanced resolution in the upper layers. But, it is also possible to adopt a more homogeneous distribution of these levels (50 in our case) along the water column, in order to gain further resolution in the subsurface and at intermediate depths (Supplementary material 2). This was achieved by setting the stretching parameters of 'theta-s' and 'theta-b' to respectively 5 and 0 and by using the newly-introduced function for the vertical coordinate transformation, with the intention of investigating the effects of tidal mechanisms on local ocean dynamics.

Taking into account that ROMS is a sigma coordinate model, a smoothing over the bathymetry, derived from the ETOPO2 *[Smith and Sandwell, 1997]* database with 2 min of resolution and a value of minimum depth at the shore (hmin) of 10 m, has been necessary to minimise pressure gradient errors. However, in order to avoid an excessive filtering of the topography, this process has been evaluated through neutral stratification tests run using an idealized stratification of the water column. This showed the need of activating the diffusive component of the advection scheme, designed to reduce artificial effects of spurious diapycnal mixing that could appear in the tracers fields (T and S).

The first mesoscale-resolving simulations were integrated for a period of 10 years, setting the output at a daily frequency, in order to evaluate not only the initial adjustment of the model but also the period necessary to achieve a statical steady-state of the simulated energy budget. The duration of this spin-up phase (about 18 months) was analysed in terms of global diagnostics of surface and volume-averaged variables: kinetic energy, vertical velocity, density, temperature and salinity (Figure 2). Then the establishment of the energy equilibrium has been examined by exploring the dynamical richness of the

simulations through the Eulerian analyses of classical variables (potential vorticity, kinetic energy, properties and volumes of the water masses, heat and salt fluxes). In the future we plan to diagnose it as well through the Langrangian tracking of the coherent, turbulent structures and the inter-basin exchanges. Further sensitivity tests of the model to realistic atmospheric forcings and lateral oceanic conditions are planned to be assessed, using inter-annual forcing for the surface atmospheric and for the lateral oceanic conditions.

In order to maximize computing efficiency of several simulations at submesoscale-permitting resolution we took advantage of the AGRIF 2-way nesting capability of ROMS. As previously mentioned, this double-nested approach is designed such that the boundary conditions of the high resolution 'child' domains are supplied by the lower resolution 'parent' domain within which they are embedded [*Debreu et al.*, 2012]. This allows for very consistent boundary conditions of the child domains than what could be obtained from, often sparsely available, in-situ data. The AGRIF 2-way nesting enables the child solutions to feed back into the parent domain and therefore allows to achieve a realistic representation of coastal and ocean dynamics at multiple, interacting scales while taking into account the "upscaling" effect.

Our two AGRIF zooms were localized over the two deltaic regions of interest, the Parnaiba and Sao Francisco (Figures 1c and 1d), and for each of them we have run 5 years-simulations at daily output of the nested configuration. The horizontal resolutions were 1/12° for the parent grid and 1/36° (~2.7 km) for the child grids, while vertically we consistently employed 50 levels, homogeneously distributed along the water column. And also in these nested solutions, we used the two previous settings: one encompassing the information of the tides components (called "Tidal") and a second one without (called "No-tide"). In terms of forcing, initial state and advection/ diffusion schemes, in the embedded grids we set exactly the same initial conditions, surface atmospheric forcing and lateral oceanic forcings (only at the parent grid boundaries) as for the single grid run (1/12°). Specific tests were also carried out for the child grid smoothing of the nested configuration.

2.2 OBSERVATIONS FOR VALIDATION

Our fist methodological step, after having run our numerical simulations, was to compare its output with the available observations of the study regions, that in our case are satellite-retrieved data, since in-situ measurements are still very sparse and rare in these areas.

In particular, we regret the lack of information on the vertical distribution of the thermo-haline and hydrodynamical variables to validate our numerical output at depth. Reason

why our model validation has the limitation of being restricted to the evaluation of the surface fields, which have been compared to satellite data analysing both their overall mean values and their seasonal cycles. For a fair comparison of the model data with the available observations, the finer resolution of the model output was degraded to approximate the lower resolution of the satellite products. Hence, the differences of several variables (sea surface salinity and temperature, zonal ad meridional current velocities, eddy kinetic energy) were computed between the mean values from the numerical output and the satellite observations (Figure 3). In the following subsection, we will briefly present the main technical aspects and oceanographic characteristics of these satellite products, as well as the websites where they can be accessed and downloaded.

2.2.1 Satellite Products

- Sea Surface Temperature (SST) product, from the TropFlux (https://incois.gov.in/tropflux/) reanalysis of air-sea heat fluxes for the global tropical oceans from 2007 to 2018: this dataset provides daily, timely, accurate air-sea heat and momentum flux data for the entire 30°N- 30°S region at 1° of spatial resolution. It is largely derived from a combination of ERA-I re-analysis data for turbulent and longwave fluxes (https://www.ecmwf.int/), and ISCCP surface radiation data for shortwave flux (https://isccp.giss.nasa.gov/). A precise description of the flux computation procedure is provided in *Praveen Kumar et al. [2012*].

- Sea Surface Salinity (SSS) from the Soil Moisture and Ocean Salinity (SMOS, https://earth.esa.int/web/guest/missions/esa-operational-eo-missions/smos) data from 2010 to 2017 at 1/3° spatial resolution. The Microwave Imaging Radiometer using Aperture Synthesis (MIRAS) radiometer picks up faint microwave emissions from Earth's surface to map levels of soil moisture, sea surface salinity, sea ice thickness and other geophysical variables such as wind speed over ocean and freeze/ thaw soil state. We used the level 2 SSS products version v662.

- U and V velocities from the Ocean Surface Current Analysis Real-time (OSCAR, https://data.planetos.com/datasets/nasa_oscar_global_5day) from 1992 to 2018: this dataset is generated by Earth Space Research (ESR, http://www.esr.org/oscar_index.html) and contains near-surface ocean current estimates, derived using quasi-linear and steady-flow momentum equations. The horizontal velocity is directly estimated from sea surface height, surface vector wind and temperature. These data, collected from various satellites and in-situ instruments, are on a 1/3° degree grid with a 5 day temporal resolution.

- Eddy Kinetic Energy (EKE = ½ [U^2 + V^2]^0.5 , *Equation 1*) estimates from the Along Track Sea Level Heights (AVISO, https://www.aviso.altimetry.fr/) from 2000 to 2016 at 1° spatial resolution: retrieved from the Ssalto/Duacs along-track altimeter products, including multi-mission sea surface heights computed with respect to a 20-year mean. Several timeliness are proposed: near-real-time and delayed-time. As well as different variables: Sea Level Anomaly and Absolute Dynamic Topography filtered and unfiltered in delayed-time. The Copernicus Marine Environment Monitoring Service (CMEMS, http://marine.copernicus.eu/) is in charge of the processing and distribution of the Sea Level Anomaly (SLA-H) and Absolute Dynamic Topography Heights (ADT-H) in the near-real-time product.

2.2 Salinity Transport across the continental platforms adjacent to the estuaries

For the estuary scales, the estimation of the salinity budget is very important for understanding the turbulent dynamics at the ocean-river interface [*Rosário et al., 2016*]. But, also at coastal and larger scales the inclusion of salinity dynamics and its variability are necessary for studying mixed and barrier layer behaviours in the western south-tropical Atlantic, where ocean-atmosphere coupling is known to be strong [*Araujo et al., 2011*]. As described in *Miranda et al. [2002]* the equation for the advective transport of salt includes at least 7 physical components, among which: the volume transport due to the river discharge; the mass transport generated by the propagation of tidal waves; the term of tidal correlation between the mean values of velocity and salinity within the water column; the transport linked to the stationary circulation, representing the difference between the gravity current and the component generated by the river discharge or residual; a term related to the oscillatory shear, to the movement due to the wind and to the turbulent fluctuations of current velocity, at a temporal scale inferior than the tidal period; a term associated to the tidal dispersion and a final term corresponding to the temporal mean of the correlation between salinity and the tides weighted by the residual velocity. *Bergamo et al. [2002]* provides a practical, computational description of this salt transport (Ts) in terms of its mean value:

$$Ts = 1/T \int_0^T \int_0^h \rho u S \, dz \, dt = \langle \overline{\rho u S h} \rangle \qquad \textit{Equation 2}$$

where 'ρ' is the water density, 'u' is the the zonal component of current velocity, 'S' is salinity, 'T' is the temporal range and 'h' is the thickness of the water column. The symbol

(<>) denotes the temporal average, while (¯) indicates the spatial mean. In general, in smaller estuaries this transport can be considered laterally homogeneous for the calculation of the advective transport of salt [*Miranda et al., 2002].* However, given the dimensions of the Sao Francisco and Parnaiba deltas, the model estimation of the salt transport would be representative just for the specific grid points chosen for the calculation. In our case, these points were selected along two transversal transects, across the continental platform, that will be used during the in-situ campaigns planned for the near-future out of the estuaries under survey and through which the flow was assumed to be laterally homogeneous. The transect is aligned to the river delta for the Parnaiba and for the Sao Francisco it is approximately traced along the canyon profile; in both cases they are placed at about 10 km from the coastline, covering a length of a couple of km and a depth of 50m. A local salt transport will be then computed and later discussed in function of the transects' positions within the simulated child grids of the two deltas as displayed in the Sea Surface Salinity maps of Figures 7a and 7 b.

3. RESULTS

The SSS, SST, U, V and EKE difference maps of Figures 3a-e, being the result of the validation of our simulations' output against satellite-retrieved observations, show how the numerical experiments that were run including the tidal components are overall able to capture the most salient aspects of the Western Tropical Atlantic circulation. In terms of the tracers' distributions, the model solution is generally marked by a positive bias in the T-S properties along the northern coast in correspondence of the Parnaiba estuary and above all of the Amazonian platform, while the modelled southern branch of the North Brazilian Current (NBC) is fresher and colder than what is observed. The root mean squared error (RMSE) mean values of the difference between the modelled properties and the observed is equal to 0.0161 for temperature and 0.0108 for salinity. These values spatially vary between the Parnaiba nested domain (0.1060 in SST and 0.0104 in SSS) and the Sao Francisco zoom (0.0593 in SST and 0.0102 in SSS). This could be due to discrepancies in the heat and salt fluxes of the two branches of the South-Equatorial Current (SEC) after bifurcation (sketched in the SST map of Fig. 3b, following [*Rodrigues et al., 2007]*).

Alike considerations can be drawn for the dynamical variables, as for the zonal and meridional components of current velocity (U and V) the RMSE mean values of the difference 'model-observations' are respectively 0.0042 and 0.0035. We see again that

more significant differences can be observed along the northern-northeastern continental shelf in particular in the vicinity of the Parnaiba estuary and along the Amazon River plume. These discrepancies are translated in a negative bias of the EKE estimation concentrated at the same locations, where the RMSE reaches a value of 0.0076 (mean value of ~0.0041). A part of them could be explained by the fact that our first, mesoscale-permitting simulation is missing the contribution of more realistic river discharge, as previously demonstrated by *Varona et al. [2019]* in a numerical study of the Amazon estuary. The qualitative findings described for the thermo-haline and dynamical variables analysed within the grid parent of the 'Tidal' simulation are similar to those extracted for the child grids of the Parnaiba and Sao Francisco rivers mouths (subplots 1 and 2 of Figures 3a-e). Apart from the mean values of the RMSE, seasonal estimates have also been computed and summarised in Table 1 for each of the 4 seasons and the 5 variables used for the model comparison with satellite data, confirming the reasonably low order of magnitude of their differences throughout the modelled 10 years of integrations.

This result is confirmed by the ROMS capacity of capturing the seasonal cycles of the thermo-haline structure (Fig. 4 a-b) within the deltas' nested domains, in comparison to the satellite observations used for the validation of the ‘Tidal’ simulation (TropFlux data for SST and SMOS data for SSS). We observe that the model has a general tendency of sub-estimating the SSS values, for which the hugest discrepancy between the monthly time series takes place in the Sao Francisco area with a difference of about 0.03 PSU between the ROMS estimate and the SMOS one. Overall, the two graphs of Figure 4 show a fair comparison between numerical results and satellite measurements, but in order to have a statistical confirmation of model ability to reproduce observations, we performed the two-sample 't-test. Prior to performing the latter, observations and numerical output were normalised since the initial dataset showed non-normal distributions as verified by the one-sample Kolmogorov-Smirnov test. Finally, the t-test results indicated no statistically significant differences between the temporal distributions of the thermo-haline variables issued of the ROMS tidal simulation and the ones retrieved from satellite data, as the values of the 'p' coefficients range from 0.9941 (for the SST in the Parnaiba zoom, Fig. 4a) to 0.9984 (for the SSS in the Sao Francisco zoom, Fig. 4b), for a significance level (α) of 0.05 in all the analysed cases.

Despite of the above-mentioned, localised discrepancies our simulations seem to be in good agreement with the regional satellite observations, while reproducing the main

mesoscale aspects and patterns of the Tropical Atlantic's Western Boundary Current.

The Potential Vorticy ($PV=\zeta a*\nabla\theta/\rho$ *Equation 3*, where 'ζa' is the absolute vorticity, 'θ' is potential temperature and 'ρ' is water density) surface maps for the parent grids of both the 'Tidal' and 'No-tide' simulations (Figs. 5a and 6a) mark the latitude (south of 10°S) at which the southern SEC (sSEC) and its central branch (cSEC) terminations form the North Brazil Undercurrent–North Brazil Current (NBUC–NBC) system. The latter represents one of the most powerful western boundary currents in the world *[Silva et al., 2009]*. The latitude where the sSEC bifurcation occurs is not well known, although it has been demonstrated from observations and model results *[Silveira et al., 1994; Stramma et al., 1995; Rodrigues et al., 2007]* that the NBUC originates south of 10°S.

The surface snapshots of PV, EKE and SST from the estuaries' zooms of Figures 5b-g and 6b-g, show that the oceanic regions adjacent to the platforms, off the rivers' deltas, are marked by the presence of small vortices, meanders and filaments probably due to the non-linear interactions between the rivers' plumes and the main currents' vortices (NBC for the Parnaiba and SEC for the Sao Francisco). These turbulent structures are visible in the maps of both the 'Tidal' and 'No-tide' simulations, even though much finer scales characterise the experiment encompassing tidal forcing, as tides are an essential process in mixing the river plumes with the open ocean *[Varona et al., 2019]*.

RMSE	Winter	Spring	Summer	Autumn
SST	0.0396	0.0279	0.0401	0.0362
SSS	0.0100	0.0181	0.0139	0.0097
U-vel	0.0047	0.0048	0.0050	0.0049
V-vel	0.0038	0.0041	0.0040	0.0037
EKE	0.0035	0.0039	0.0042	0.0043

Table 1: RMSE values between the satellite observations described in Section 2.2.1 and the output of the 1/12° simulation with 50 levels in terms of Sea Surface Temperature (SST, 1st row), Sea Surface Salinity (SSS, 2nd row), zonal and meridional velocities (U-vel and V-vel, respectively 3rd and 4th rows), Eddy Kinetic Energy (EKE, 5th row).

Part of the meso-submesoscale dynamics could be indeed attributed to the interactions of tidal waves with local bathymetry and with some of the SEC central and southern terminations, as documented in previous numerical and observational studies *[Silva et al., 2009b, 2010; Coles et al., 2013; Korosov et al., 2015; Newinger and Toumi, 2015; Araujo et al., 2017].* The differences between the two numerical configurations ('Tidal' and 'No-tide' setups) were quantified calculating the RMSE values in terms of PV, EKE and SST for

the parent grid and for the Parnaiba and Sao Francisco zooms (Table 2), showing that important discrepancies are especially present in the reproduction of the temperature distribution and thus of the overall PV budget.

Model Domain	RMSE in PV	RMSE in EKE	RMSE in SST
Parent Grid	1.2445	0.004	1.1282
Parnaiba zoom	0.9193	0.0185	2.198
Sao Francisco zoom	1.0274	0.0035	1.9943

Table 2: RMSE values between the 'Tidal' and 'No-tide' configurations of the 1/12° simulation with 50 levels (1st row) and between the nested zooms at 1/36° embedded within them (2nd and 3rd rows) for different variables: Potential Vorticity (PV, 1st column), Eddy Kinetic Energy (EKE, 2nd column) and Sea Surface Temperature (SST, 3rd column).

The effects of the tidal forcing inclusion in the model on the dynamical processes typical of estuarine- coastal regions can also be qualified through the analysis of the salt transports' time series displayed in Figure 7c. In this plot, the calculation of the daily mean transport of salt was carried out using the output of the model last year (Y10) of both the 'Tidal' and 'No-tide' nested simulations. These averaged values were extracted along the two transects localised across the continental platforms adjacent to the Parnaiba and Sao Francisco estuaries (respectively Figure 7a and 7b), representing the possible positions of stations to use during the oceanographic surveys planned in these regions in the near-future. The 'Tidal' and 'No-tide' curves of these mean salt transports (respectively continuous and dotted lines in Figure 7c) show similar patterns and generally positive values for the Parnaiba River and negative ones for the Sao Francisco. However, the 'No-tide' estimates are marked by much lower values for both rivers, highlighting how the tidal forcing plays an important role in the horizontal distribution and advection of salt within the coastal areas closed to the estuaries of interest. This is in accordance with the numerical findings of *Wey et al. [2014]* for most types of estuaries, revealing that the leading order residual salt transport is driven by horizontal diffusion, river outflow, and tidal advection.

In the case of the 'Tidal' experiment, to better investigate the influence of this forcing on the behaviour of the dynamical variables at depth, instantaneous zonal and meridional sections of current velocities were extracted along the same sections, placed across the continental shelf near the deltas, where the salt transport time series were estimated. These velocity sections are shown in Figures 8a-d, where positive (negative) values indicated by solid (dashed) lines correspond to north-westward (south-eastward) currents. In these plots, both the Parnaiba and the Sao Francisco coastal areas seem to be

interested by an intense eddy activity, since cyclones and anticyclones alternate below the sea surface, and some of them have an important vertical structure that can be traced down to 1500 m of depth. In case of the Sao Francisco, morphologically characterised by a deep canyon, the eddies' extension along the water column is more significant, reaching a mean depth of almost 2000 m. This points out to the possible formation of subsurface-intensified mesoscale features. That is why it was necessary to increase the numerical resolution within the embedded child grids, in order to become fully mesoscale-resolving and even submesoscale-permitting both in the horizontal and in the vertical.

This eddy activity can be better traced at depth by plotting instantaneous profiles of relative vorticity 'ζ' (Figure 9a), extracted at the locations where current velocity assumes its greatest magnitude at the surface in each of the two child grids (indicated by a black star in the velocities' sections of Figures 8a and 8c) and comparing the behaviour of the 'Tidal ' and 'No-tide' runs also in the vertical (RMSE values between the two estimates are about 3.8 for the Sao Francisco and 2.7 for the Parnaiba). For both the Sao Francisco and Parnaiba deltas, the 'Tidal' and 'No-tide' profiles have, almost at all depths, an opposite sign, although in the case of the 'No-tide' run the excursion of positive and negative values is more reduced. However, for both the configurations and deltas these profiles suggest an alternation of anticylonic and cyclonic eddies, whose effects in thermo-haline properties is vertically less marked than their dynamical signature. Indeed, the T-S diagrams of Figure 9b show for both deltas slight discrepancies between the two configurations, since the RMSE estimates between the 'Tidal' and 'No-tide' curves are approximately 0.05 for the Sao Francisco and 0.1 for the Parnaiba.

To further assess the differences between the two deltaic regions of interest in terms of the tidal forcing we have performed some diagnostics regarding its local elevation, the regional distribution of the major tidal components and the approximation of the tidal wave on the continental platforms adjacent to the rivers' deltas. We primarily traced a time series of the tidal range from the first 20 days of the model integration, extracting the values of sea level from the TPX07 product used to force the model at the coastal gauge stations closest to each one of the two estuaries (Supplementary Material 3). This graph points out how the two deltas are interested by a very similar, semi-diurnal period even though the tidal range is greater in the Parnaiba area. This slight distinction is visible also in the surface maps of the first, four tidal constituents among the ten considered in our tidal simulation (**M2, S2, N2, K2,** K1, O1, P1, Q1, Mf, Mm) showing higher values along the Parnaiba coastline for each of the displayed constituents. But, at the regional scale, not huge discrepancies can

be observed between the two deltas in terms of the overall intensity of these tidal components. Then zooming to finer scales, more significant differences can be noted. Indeed, in the plots of the M2 (major semi-diurnal lunar component) tidal amplitude and phase extracted within the nested domains of each delta (Figure 10 'a-d'), we observe that much lower intervals of values are present in the Sao Francisco area, where the tidal ellipse (mathematical approximation of the tidal wave) shape is almost point-like. Instead, close to the Parnaiba delta the tidal ellipse has a well-defined shape, turning and flattening its axis in proximity of the continental platform where the magnitude of the M2 tidal amplitude and phase substantially increase (note the different ranges of values between the colour bars of Figure 10 a-c and b-d).

4. DISCUSSION AND CONCLUSIONS

Besides the fact that the model accurately reproduces the satellite-derived variables overall (SSS, SST, U and V velocities, EKE of Figures 3a-e) and the thermo-haline seasonal cycles (Figures 4a-b), it also resolves the local mesoscale dynamics quite well, including frontal structures, meanders and specific upwelling regions. For instance, the concentration of tiny filaments observed in the model PV map of Figure 5a in the vicinity of the Abrolhos Bank (Lat. 17–18°S—Long. 38.5°0 –39.5°W, marked by a black asterisk) and the Vitória-Trindade Ridge (Lat. 20°S—Long. 34–38°W, marked by a black square) are good hints of observed and modelled upwelled, cold waters and mesoscale cyclonic structures previously documented in this area *[Schmid et al., 1995; Campos, 2006]*. In fact, the modelled SST and EKE are especially efficient compared to the satellite estimates of these variables in proximity of the coastline (~10 km), where the infrared and the altimetric retrievals may be respectively cloud-contaminated and limited by the data gaps along the continental shelf.

The capacity of the ROMS model to capture the fine-scale, turbulent structures has been proved in both the 'Tidal' and 'No-tide' configurations, as evidenced in the nested maps of PV, EKE and SST (Figures 5b-g and 6b-g). Even though for a thorough analyses of the dynamical differences between these two numerical setups both simulations should be rerun with output at hourly frequency, we can already observe some evident discrepancies in the distribution of the potential vorticity, eddy kinetic energy and temperature shown in their surface maps, which were quantified in terms of the RMSE values of Table 2.

Significant differences between the two configurations emerge as well in the time series of salt transport of Figure 7c, which relates the movement of salt along an estuarine channel

to several physical forcings (e.g., tides, freshwater flow, wind). The latter relationship is essential in predicting the extent of saline intrusion within the estuary and provides insight into the dispersal of other substances *[Monismith et al.,1996; Wells and Young, 1992].* Salt transport is generally divided into a seaward advection of salt, due to the net river outflow and two mechanisms of landward salt transport, the estuarine salt transport (i.e., the vertical and lateral variations of tidally averaged, or ‘‘residual,’’velocity and salinity) and tidal dispersion (i.e., the tidal correlations of velocity and salinity) *[Fischer, 1976]*. Generally the calculation of properties' transport is realized along a section transversal to the estuary, once considered the estuary laterally homogeneous *[Bergamo et al., 2002; Miranda et al. 2002; Vaz et al., 2012]*. In the case of the Sao Francisco and Parnaiba rivers, taken into account their reasonable width, their estuaries were not considered so. Thus, the salt transports shown in the time series of Figures 7c were calculated along two transects localised across the continental platforms adjacent to the estuaries of interest (Figs. 7a and 7b), where the hypothesis of lateral homogeneousness of the flow was assumed. For most of the analysed year (model Y10), the two mean estimates of salt transport had mainly an opposite sign, being negative in the case of the Sao Francisco and positive for the Parnaiba. In-situ mesurements of such physical quantity would be required to locally explain the dynamical processes that influence this contrasted behaviour. But at a larger scale, we could hypothesize that this is related to a higher rate of evaporation characterising the coastal area off the Parnaiba delta, geographically placed more northeast than the Sao Francisco estuary *[Hastenrath, 2006]*.

Another reason could be represented by the northward transport of warmer and saltier waters by the NBC's rings, which have a vertical signature as significant as the horizontal one. Indeed, in the vertical sections of the meridional and zonal velocities extracted from the 'Tidal' simulation (Figures 8a-d), eddies of both signs, at times appearing as dynamical dipoles, can be traced at meaningful depths, which, in the case of the Sao Francisco canyon, can get down to 2000 m. The existence of subsurface mesoscale vortices associated to the NBC retroflection is, in some areas of the two nested domains, evidenced without any signature in the surface layer, so confirming earlier model outputs [*Silva et al., 2009b*]. Those of them which are subsurface anticyclones (also named 'rings' in the regional literature), linked to the NBC/NBUC retroflection into the north Equatorial Undercurrent (nEUC) and the EUC, contribute to the transport of South Atlantic high salinity water into the Northern Hemisphere. The numerical results of *Silva et al. [2009b*] highlighted that, during all the seasons, the Salinity Maximum Waters (SMWs) coming

from the North Atlantic are transported through the boundaries of these rings (near 8°N), while the SMWs coming from the South Atlantic are transported within the core of the rings during their north-westward displacement. In a similar way, *Johns et al. [2003]* described in the Western Tropical Atlantic the presence of intensified subsurface rings above the thermocline but without any signature at the surface. These structures were also reproduced in the modelling works of *Barnier et al. [2001], Garraffo et al. [2003]*, and *Stramma et al. [2005]*. More recent observations of the North Brazil Current Rings (NBCR) Experiment *[Johns et al., 2003]* confirmed the existence of a ranking of surface and subsurface NBC rings between 50 and 40°W, transporting SAW on the ring core and North Atlantic Water (NAW) on its boundaries. They would represent the third type of NBC rings described by *Wilson et al. [2002],* namely thermocline intensified structures with almost no detectable surface signature, as emerged in the nested velocity sections of Figures 8 (a-d) and in the relative vorticity profiles of Figure 9a. In these latter plots, the dynamical signature of anticyclonic and cyclonic eddies at depth is much greater than in the upper layers. In contrast, T-S variations are more significant near the surface (Figure 9b), even though their behaviour does not substantially differ between the 'Tidal' and 'No-tide' configurations as much as seen in the curves of relative vorticity. This suggests that the numerical inclusion of the tidal forcing has a greater impact on the eddy dynamics than on the thermo-haline structure of the simulated regions of study.

To further characterize the difference of the tide influence between the two estuaries, a set of tidal metrics (plots of the range and of the 4 major components' amplitudes in the Supplementary Material 3 and 4; M2 amplitude, phase and ellipse of the tidal wave in Figure 10 a-d) were computed from the model and analysed within the nested domain of each delta. The Parnaiba case shows much higher values of tidal elevation, amplitudes of the four tidal constituents taken into account and also in terms of the M2 parameters and ellipse, than the Sao Francisco area. This tidal difference could represents one of the reasons why the subsurface variations of RV are more pronounced in the Parnaiba profiles than in the Sao Francisco ones. And it could also explain the greater magnitude of the PV values along the Parnaiba continental platform than within the Sao Francisco region.

In addition to the presence of the cited surface and subsurface eddies in the regions of study, another source of turbulence could be represented by the interaction of these mesoscale structures with the rivers plumes and tidal-estuarine processes, particularly effective within canyons, where turbulence is usually orders of magnitude stronger than in the open ocean *[Nash and Moum, 2001; Kunze et al., 2002].* These interactions may

include: (i) internal wave critical reflection *[Eriksen, 1982];* (ii) scattering of the barotropic tide and internal waves off small-scale topography *[St. Laurent and Garrett, 2002];* (iii) internal lee wave generation by small scale topography *[Thorpe 1996];* and (iv) eddy shedding *[MacCready and Pawlak, 2001]*. For the time being, the multiple limitations of our numerical work does not allow to evaluate if the interaction of the river plume with (iv) could be one of the mechanisms taking place in the areas of interest or rather due to the (iii) type of mechanism. Specific, process-oriented studies would be needed to evaluate the role played by each of the above-mentioned interactions within the two areas of interest, but such an insightful research goes beyond the scopes of the current paper. Moreover, high-resolution sampling in both time and space are required to resolve and to analyse the scales of the listed processes inside canyons *[Solé et al., 2016]* and within the continental platforms under investigation.

In summary, for the oceanic region of study, ROMS provides a numerically exhaustive description of the coastal, estuarine processes and their properties' variabilities. Our numerical results, coming from regional climatological modelling, are in good agreement with previous studies and satellite-retrieved observations, showing similar patterns of thermo-haline distribution and ocean surface circulation of the Western Tropical Atlantic. At present, our findings provided evidence of an intense turbulent activity characterising the T-S structure and hydrodynamical regimes of two among the main estuaries of the Northeastern Brazil: the Sao Francisco and Parnaiba rivers. Embedded child grids, run within their coastal areas and adjacent platforms at much higher resolution than the original parent grid, allowed to qualify in more details the fine-scale interactions between the river's plume and the SEC terminations, in the case of the Sao Francisco (PV maps of Figs. 5a and 5e), and with the passage of the NBC rings, for the Parnaiba. Therefore, the dynamics of both deltas are marked by short spatio-temporal scales of variability in terms of the main patterns of circulation, hydrodynamical properties and thermo-haline structure. This is reflected also in the vertical sections of the current velocities, where it looks like the Sao Francisco shelf and adjacent platform is interested by the presence of subsurface-intensified eddies (Fig. 8 c-d). Similarly, a strong turbulence seems to characterise the oceanic region off the Parnaiba delta, both at surface (Fig. 5 b-d) and at depth (Fig. 8 a-b). In order to investigate in more details all these processes in the next future, the current model configuration will be improved by using a higher resolution and including finer, dynamical scales, better turbulence closure schemes, and more realistic products for the surface forcing and lateral boundary conditions. Using the

nesting capability of ROMS, we will continue to explicitly resolve the fast propagating signals across the whole Tropical Atlantic while addressing the coastal response within the regions of the embedded child grids. Another further step would be the comparison of the simulations' output with in-situ data. The availability of accurate observations for the model comparison will allow us to run offline Lagrangian integration of particles in order to quantify currents' trajectories in more details, as well as to describe tracers' pathways within the estuaries of interest and along the adjacent continental platforms.

AKNOWLEDGEMENTS

The authors greatly appreciate the graphical help from Carlos Noriega and the technical aid from Fabiana Soares based at the CEERMA (Centro de Estudos e Ensaios em Risco e Modelagem Ambiental) institute of the Federal University of Pernambuco (UFPE). We acknowledge: the CAPES PNPD Brazilian scholarship (Portaria 086/2013) for having supported the author's research as post-doctoral fellow at UFPE; the LAPECO conference (https://lapeco2019.blogspot.com) for the opportunity of submitting this work as a Special Issue; and the INCT AmbTropic project (http://inct.cnpq.br/web/inct-ambtropic), providing the scientific framework for this study. We thank the IT team of the LEGOS lab for their precious advices on different aspects of the model implementation on their server and the IDRIS assistance for their support. And a special thank goes to the two reviewers who helped us improving this manuscript.

REFERENCES

- Almeida Filho, R.; Rossetti, D.F.; Miranda, F.P.; Ferreira, F.J.; Silva, C., and Beisl, C., 2009. Quaternary reactivation of a basement structure in the Barreirinhas Basin, Brazilian Equatorial Margin. Quaternary Research, 72(1), 103–110.

- Antonov, J., Seidov, D., Boyer, T., Locarnini, R., Mishonov, A., Garcia, H., Baranova, O., Zweng, M., Johnson, D., 2010. World Ocean Atlas 2009. In: In: Levitus, S. (Ed.), Salinity, vol. 2. NOAA Atlas NESDIS 69, pp. 184.

- Aquino da Silva, A.G.; Stattegger, K.; Schwarzer, K.; Vital, H., and Heise, B., 2015. The influence of climatic variations on river delta hydrodynamics and morphodynamics in the Parnaíba Delta, Brazil. Journal of Coastal Research, 31(4), 930–940. Coconut Creek (Florida), ISSN 0749-0208.

- Aquino da Silva, A.G.; Stattegger, K.; Schwarzer, K.; Vital, H., and Heise, B., 2019. Coastline change and offshore suspended sediment dynamics in a naturally developing delta (Parnaíba Delta, NE Brazil). Mar Geol 410:1–15.

- Araujo, M., Limongi, C., Servain, J. et al., 2011. Salinity-induced mixed and barrier layers in the Southwestern tropical Atlantic Ocean off the Northeast of Brazil. Ocean Science, vol. 7, no. 1, pp. 63–73.

- Araujo, M., Noriega, C., and Lefèvre, N., 2014. Nutrients and carbon fluxes in the estuaries of major rivers flowing into the tropical Atlantic. Front. Mar. 1:10. doi: 10.3389/fmars.2014.00010

- Araujo, M., Noriega, C., Hounsou-Gbo, G.A., Veleda, D., Araujo, J., Bruto, L., Feitosa, F., Flores-Montes, M., Lefèvre, N., Melo, P., Otsuka, A., Travassos, K., Schwamborn, R., Neumann-Leitão, S., 2017. A synoptic assessment of the amazon river-ocean continuum during boreal autumn: from physics to plankton communities and carbon flux. Front. Microbiol. https://doi.org/10.3389/fmicb.2017.01358.

- Araújo, H.A.B., Dominguez, J.M.L., Machado, A.J., Rangel, A.G.A.N., 2018. Benthic foraminifera distribution in a deltaic clinoform (São Francisco Delta, eastern Brazil): A reference study. Journal of marine Systems 186:1-16.

- Barnier, B., Reynaud, T., Beckmann, A., Boning, C., Molines, J.- M., Barnard, S., and Jia, Y., 2001. On the seasonal variability and eddies in the North Brazil Current: insight from model inter-comparison experiments, J. Progress in Oceanogr., 44, 195–230.

- Bérgamo A. L., Miranda L. B., Corréa M. A., 2002. Estuário: Programas para processamento e análise de dados hidrográficos e correntográficos. Relat. Téc. Inst. Oceanogr., (49):1-16. Universidade de São Paulo, Instituto Oceanográfico.

- Bernardes, M. C.; Knoppers, B. A.; Rezende, C. E.; Souza, W. F. L.; Ovalle, A. R. C. Land-sea interface features of four estuaries on the South America Atlantic coast. Brazilian Journal of Biology = Revista Brasileira de Biologia, v. 72, n. 3, p. 761-774, 2012. Supplement. PMid:23011302. http://dx.doi.org/10.1590/S1519-69842012000400011.

- Bhattacharya, J.P., Giosao, L., 2003. Wave-influenced deltas: geomorphological implications for facies reconstruction. Sedimentology 50, 187–210.

- Bittencourt, A.C.S.P., Dominguez, J.M.L., Martin, L., Ferreira, Y.A., 1982. Dados Preliminares sobre evolução do delta do Rio São Francisco (SE/AL) durante o quaternário: influência das variações do nível do mar. In: Proceedings VI Simpósio do Quaternário no Brasil, pp. 46–68.

- Bittencourt, A.C.S.P., Dominguez, J.M.L., Martin, L., Silva, I.R., 2005. Longshore transport on the northeastern Brazilian coast and implications to the location of large scaleaccumulative and erosive zones: an overview. Mar. Geol. 219, 219–234. http://dx.doi.org/10.1016/j.margeo.2005.06.006.

- Bittencourt, A.C.S.P., Dominguez, J.M.L., Fontes, L.C.S., Sousa, D.L., Silva, I.R., Da Silva , F.R., 2007. Wave refraction, river damming, and episodes of severe shoreline erosion: The São Francisco River mouth, northeastern Brazil. Journal of Coastal Research, 23(4), 930–938. West Palm Beach (Florida), ISSN 0749-0208.

- Bianchi, T.S. and Allison, A. M., 2009. Large-river delta-front estuaries as natural "recorders" of global environmental change. Proceedings of the National Academy of Sciences May 2009, 106 (20) 8085-8092; DOI: 10.1073/pnas.0812878106.

- Blayo, E., Debreu, L., (1999). Adaptive mesh refinement for finite-difference ocean models: First experiments. Journal of Physical Oceanography 29, 1239-1250.

- Bourlès, B., Molinari, R.L., Johns, E., Wilson, W.D., Leaman, K.D., 1999a. Upper layer currents inthe western tropical North Atlantic (1989-1991). Journal of Geophysical Research 104, 1361–1375.

- Campos, E.J.D., 2006. The equatorward translation of the Vitoria eddy in a numerical simulation. Geophysical Research Letters 33, L22607. Doi:10.1029/ 2006GL026997.

- Cavalcante, G., Miranda, L. B. de, & Medeiros, P. R., 2017. Circulation and salt balance in the Sao Francisco river Estuary (NE/Brazil). *RBRH*, *22*, e31. Epub April 10, 2017.https://doi.org/10.1590/2318-0331.021720170003.

- Coles, V.J., Brooks, M.T., Hopkins, J., Stukel, M.R., Yager, P.L., Hood, R.R., 2013. The pathways and properties of the Amazon river plume in the tropical North Atlantic Ocean. Journal of Geophysical E Research C: Oceans 118, 6894–6913.

- Da Silva, A., Young, A.C., Levitus, S., 1994. Atlas of sur face marine data 1994. Algorithms and Procedures. Technical Report 6, vol. 1 NOAA, NESDIS.

- Dai, A., Trenberth, K.E., 2002. Estimates of freshwater discharge from continents: latitudinal and seasonal variations. J. Hydrometeorol. 3, 660–687. https://doi.org/ 10.1175/1525-7541.

-Debreu, L., Vouland, C., 2003. AGRIF: Adaptive Grid Refinement in Fortran.[Available online http://www-lmc.imag.fr/IDOPT/AGRIF/index.html].

-Debreu, L., Mazauric, C., 2006. Adaptive Grid Refinement (AGRIF) in Fortran 90: Users Guide Version 1.3. <http://www-lmc.imag.fr/IDOPT/AGRIF/index.html>.

-Debreu, L., Blayo, E., 2008. Two-way embedding algorithms: a review. Ocean Dyn. 58, 415–428.

- Dengler, M., F. A. Schott, C. Eden, P. Brandt, J. Fischer, and R. Zantopp, 2004: Break-up of the Atlantic deep western boundary current into eddies at 8°S. Nature, 432, 1018–1020.

- De Paula Filho, F. J., Lacerda, L. D., Marins, R. V., Aguiar, J. E., & Peres, T. F., 2015. Backgroud valaues for evaluation of heavy metal contamination in sediments in the Parnaíba River Delta estuary NE/Brazil. *Marine Pollution Bulletin, 91*, 424–428.

- Dominguez, J.M.L., Martin, L., Binttencourt, A.C.S.P., 1987. Sea-level history and quaternary evolution of river mouth-associated beach-ridge plains along the East-Southeast Brazilian coast: a summary. In: Sea-Level Fluctuations and Coastal Evolution, pp. 115–127. http://dx.doi.org/10.2110/pec.87.41.0115.

- Dominguez, J.M.L., 1996. The São Francisco Strandplain: a paradigm for wave-dominated deltas? In: De Batist, M., Jacobs, P. (Eds.), Geology of Siliciclastic Shelf Seas, pp. 217–231 London, England.

- Donner S. D., Kucharik C. J., Foley J. A. , 2004. Impact of changes in land use practices on nitrate export by the Mississippi River. Global Biogeochemci.18, doi:101029/2003GB002093.

-D'Onofrio, E., Oreiro, F., Fiore, M., 2012. Simplified empirical astronomical tide model—an application for the Río de la Plata estuary. Comput. Geosci. 44, 196–202.

- Egbert, G.D., Bennett, A.F., Foreman, M.G.G., 1994. TOPEX/POSEIDON tides estimated using a global inverse model. J. Geophys. Res. Oceans 99, 24821–24852.

- Egbert, G.D., Erofeeva, S.Y., 2002. Efficient inverse modeling of barotropic ocean tides. J. Oceanic Atmos. Technol. 19, 183–204.

- Eyring, V., Bony, S., Meehl, G. A., Senior, C. A., Stevens, B., Stouffer, R. J., and Taylor, K. E., 2016. Overview of the Coupled Model Intercomparison Project Phase 6 (CMIP6) experimental design and organization, Geosci. Model Dev., 9, 1937-1958, doi:10.5194/gmd-9-1937-2016.

-Eriksen, C. C., 1982. Observations of internal wave reflection off sloping bottoms. J. Geophys. Res., 87, 525–538.

- Ferry, N., Reverdin, G., 2004. Sea surface salinity interannual variability in the western tropical Atlantic: An ocean general circulation model study. Journal of Geophysical Research: Oceans 109, 1–11. doi:10.1029/2003JC002122.

- Fischer, H. B., E. John List, R. C. Y. Koh, J. Imberger, and N. H. Brooks, 1979. Mixing in Inland and Coastal Waters, 483 pp., Academic, San Diego,Calif.

- Galloway, W. E., 1975. Process framework for describing the morphologic and stratigraphic evolution of deltaic depositional systems. In: Broussard, M.L. (ed.), Deltas, Models for Exploration. Houston, Texas: Houston Geological Society.

- Garraffo, Z. D., Johns, W. E., Chassignet, E. P., and Goni, G. J., 2003. North Brazil Current rings and transport of southern water in a high resolution numerical simulation of the North Atlantic, in: Interhemispheric Water Exchanger in the Atlantic Ocean, edited by: Goni, G. J. and Malanotte-Rizzoli, P., Elsevier Oceanographic Series, 68, 375–409.

- GEBCO, 2003. Centenary edition of the GEBCO Digital Atlas, Intergovernmental Oceanographic Commission, International Hydrographic Organization, and British Oceanographic Data Centre. Liverpool, U. K.

- Gorelick, N., Hancher, M., Dixon, M., Ilyushchenko, S., Thau, D., & Moore, R., 2017. Google Earth Engine: Planetary-scale geospatial analysis for everyone. Remote sensing of Environment, 202, 18-27.

- Grodsky, S.A., Reul, N., Lagerloef, G., Reverdin, G., Carton, J.A., Chapron, B., Quilfen, Y., Kudryavtsev, V.N., Kao, H.Y., 2012. Haline hurricane wake in the Amazon/Orinoco plume: AQUARIUS/SACD and SMOS observations. Geophysical Research Letters 39, 4–11.

- Hastenrath, S., 2006. Circulation and teleconnection mechanisms of Northeast Brazil droughts. Progess in Oceanography, 70(2–4), 407– 415.

- Hu, C., Montgomery, E.T., Schmitt, R.W., Muller-Karger, F.E., 2004. The dispersal of the Amazon and Orinoco River water in the tropical Atlantic and Caribbean Sea: Observation from space and S-PALACE floats. Deep Sea Research Part II: Topical Studies S in Oceanography 51, 1151–1171.

- Ibánhez, J.S.P., Flores, M., Lefèvre, N., 2017. Collapse of the tropical and subtropical North Atlantic CO2 sink in boreal spring of 2010. Scientific Reports 7, 41694.doi:10.1038/srep41694.

- Johns, W. E., Zantopp, R. J., and Goni, G. J., 2003. Cross-gyre watermass transport by North Brazil Current Rings, in: Interhemispheric Water Exchanger in the Atlantic Ocean, edited by: Goni, G. J. and Malanotte-Rizzoli, P., Elsevier Oceanographic Series, 68, 411–441, ISBN 0-444-51267-5.

- Knoppers, B., Weber, R.P.M., Jennerjahn, T., 2006. The São Francisco estuary Brazil. Hdb Env Chem. 5 (Part H), 51–70. http://dx.doi.org/10.1007/698_5_026.

- Korosov, A., Counillon, F., Johannessen, J.A., 2015. Monitoring the spreading of the Amazon freshwater plume by MODIS, SMOS, Aquarius, and TOPAZ. Journal of Geophysical Research C: Oceans 120, 268–283

- Kundzewicz Z. W., et al. 2008. The implications of projected climate change for freshwater resources and their management. Hydrol Sci 53:3–10.

- Kunze, E., L.K. Rosenfeld, G.S. Carter, and M.C. Gregg, 2002. Internal Waves in Monterey Submarine Canyon. *J. Phys. Oceanogr.,* 32, 1890–1913, https://doi.org/10.1175/1520-0485(2002)032<1890:IWIMSC>2.0.CO;2.

- Landim Dominguez, J. M., Pereira da Silva, R., Sá Nunes, A., Menezes Freire, A. F., 2012. The narrow, shallow, low-accommodation shelf of central Brazil: Sedimentology, evolution, and human uses. Geomorfology Vol. 23, p. 46- 59.

- Lefèvre, N., Diverrès, D., Gallois, F., 2010. Origin of undersaturation in the western tropical Atlantic. Tellus B 62, 595–607.

- Locarnini, R., Mishonov, A., Antonov, J., Boyer, T., Garcia, H., Baranova, O., Zweng, M., Johnson, D., 2010. World Ocean Atlas 2009. In: In: Levitus, S. (Ed.), Temperature, vol. 1 US Gov. Print. Off., Washington, DC 184 pp.

- MacCready, P., and G. Pawlak, 2001. Stratified flow along a corru- gated slope: Separation drag and wave drag. J. Phys. Oceanogr., 31, 2824–2839.

- Marengo, J.A., Chou, S.C., Kay, G., Alves, L.M., Pesquero, J.F., Soares, W.R., Santos, D.C., Lyra, A.A., Sueiro, G., Betts, R., Chagas, D.J., Gomes, J.L., Bustamante, J.F., Tavares, P., 2012. Development of regional future climate change scenarios in South America using the Eta CPTEC/HadCM3 climate change projections: climatology and regional analyses for the Amazon, São Francisco and the Paraná River basins. Clim. Dyn. 38, 1829–1848.

- Miranda L. B., Castro B. M., Kjerfve B., 2002. Princípios de Oceanografia Física em Estuários. 2a ed. Edusp, São Paulo, 426 p.

- Monismith, S., J. R. Burau, and M. Stacey, 1996.Stratification dynamics andgravitational circulation in northern San Francisco Bay, inSan FranciscoBay, the Ecosystem, edited by J. T. Hollibaugh, pp. 123–153, AAASPress, Washington D. C.

- Nash, J. D., and J. N. Moum, 2001. Internal hydraulic flows on the continental shelf: High drag states over a small bank. J. Geophys. Res., 106, 4593–4611.

- Newinger, C., Toumi, R., 2015. Potential impact of the colored Amazon and Orinoco plume on tropical cyclone intensity. J. Geophys. Res. Oceans 120, 1296–1317.

- Nittrouer C., and Demaster, J. (1996). The Amazon shelf setting: tropical, energetic, and influenced by a large river. Cont. Shelf Res. 16, 553–573. doi: 10.1016/0278-4343(95)00069-0

- Penven, P., Debreu, L., Marchesiello, P., McWilliams, J.C., (2006). Application of the ROMS embedding procedure for the central California upwelling system. Ocean Model. 12, 157–187.

- Praveen Kumar, B., Vialard, J., Lengaigne, M. *et al.* TropFlux: air-sea fluxes for the global tropical oceans—description and evaluation. *Clim Dyn* **38,** 1521–1543 (2012). https://doi.org/10.1007/s00382-011-1115-0.

- Praveen Kumar, B., Vialard, J., Lengaigne, M. *et al.* TropFlux wind stresses over the tropical oceans: evaluation and comparison with other products. *Clim Dyn* **40,** 2049–2071 (2013). https://doi.org/10.1007/s00382-012-1455-4.

- Rangel, A.G.A.N., 2017. Sedimentação e arquitetura deposicional do delta do São Francisco utilizando sísmica rasa de alta resolução (Undergraduate thesis). Federal University of Bahia, Brazil (48p.).

- Rangel, A.G.A.N., Dominguez, J.M.L., 2015. Sedimentation and depositional architecture of the delta of the São Francisco River using high-resolution seismic data. In: Proceedings, 14th International Congress of the Brazilian Geophysical Society & EXPOGEF, Rio de Janeiro, Brazil, (not sequentially numbered).

- Reading, H.G. and Collinson, J.D., 1996. Sedimentary Environments: Processes, Facies and Stratigraphy. Oxford: Blackwell Science, 704p.

- Rodrigues, R.R., Rothstein, L.M., Wimbush, M., 2007. Seasonal variability of the South

Equatorial Current bifurcation in the Atlantic Ocean: a numerical study. Journal of Physical Oceanography 37, 16–37.

- Rosário RP, Borba TAC, Santos AS, Rollnic M (2016) Variability of Salinity in Pará River: 2D Analysis with Flexible Mesh Model. In: Vila-Concejo, A.; Bruce, E.; Kennedy, D.M.,and McCarroll, R.J. (eds.), Proceedings of the 14th International Coastal Symposium (Sydney, Australia). Journal of Coastal Research, Special Issue, 75: 128–132.

- Schmid, C., Schafer, H., Podesta, G., Zenk, W., 1995. The Vitoria eddy and its relation to the Brazil Current. Journal of Physical Oceanography 25, 2532–2546.

- Schmitz Jr., W.J., McCartney, M.S., 1993. On the North Atlantic Circulation. Reviews of Geophysics 31, 29–49.

-Shchepetkin, A. F., and J. C. McWilliams (2003), A method for computing horizontal pressure-gradient force in an oceanic model with a nonaligned vertical coordinate.Geophys. Res.108(C3), 3090, doi:10.1029/ 2001JC001047.

- Shchepetkin, A.F., McWilliams, J.C., 2005. The regional oceanic modeling system (ROMS): a split-explicit, free-surface, topography-following-coordinates oceanic model. Ocean Modelling 9, 347–404.

- Silva, A. C., Araujo, M., Medeiros, C., Silva, M., Bourlès, B., 2005. Seasonal changes in the mixed and barrier layers in the western equatorial Atlantic. Brazilian Journal of Oceanography 53(3/4), 83-98.

- Silva, M., Araujo, M., Servain, J., Penven, P., Lentini, C.A.D., 2009a. High-resolution regional ocean dynamics simulation in the southwestern tropical Atlantic. Ocean Modelling 30, 256–269.

- Silva, A. C., Bourlès, B., Araujo, M., 2009b. Circulation of the thermocline salinity maximum waters off the Northern Brazil as inferred from in situ measurements and numerical results. Annales Geophysicae 27, 1861-1873.

- Silva, A. C., Araujo, M., Bourlès, B., 2010. Seasonal variability of the Amazon River plume during REVIZEE Program. Tropical Oceanography 38, 70-81.

- Silveira, I.C.A., Miranda, L.B., Brown, W.S., 1994. On the origins of the North Brazil Current. Journal of Geophysical Research 99, 22501–22512.

- Smith, W.H.F., Sandwell, D.T., 1997. Global sea floor topography from satellite altimetry and ship depth soundings. Science 80- (277), 1956–1962.

- Solé J., Emelianov M., Ostrovskii A., Puig P., García-Ladona E. 2016. Fine-scale water mass variability inside a narrow submarine canyon (the Besòs Canyon) in the NW Mediterranean Sea. Sci. Mar. 80S1: 195- 204. doi: http://dx.doi.org/10.3989/scimar.04322.05A

- St. Laurent, L., and C. Garrett, 2002. The role of internal tides in mixing the deep ocean.

J. Phys. Oceanogr., in press.

- Stramma, L., Fischer, J., Reppin, J., 1995. The North Brazil Undercurrent. Deep Sea Research I 42, 773–795.

- Stramma, L., Rhein, M., Brandt, P., Dengler, M., Böning, C., Walter, M., 2005. Upper ocean circulation in the western tropical Atlantic in boreal fall 2000. Deep Sea Research Part I: Oceanographic Research Papers 52, 221–240.

- Thorpe, S. A., 1996. The cross-slope transport of momentum byinternal waves generated by alongslope currents over topography. J. Phys. Oceanogr., 26, 191–204.

- Varona Gonzalez, H., Veleda, D., Silva, M. Cintra, M., Araujo, M. 2019. Amazon River plume influence on Western Tropical Atlantic dynamic variability. Dynamics of Atmospheres and Oceans. 85. 1-15. 10.1016/j.dynatmoce.2018.10.002.

- Vaz N., Lencart, Silva J. D., Dias J. M., 2012. Salt Fluxes in a Complex River Mouth System of Portugal. PLoS ONE 7(10): e47349.

- Veleda, D., Araujo, M., Zantopp, R., Montagne, R., 2012. Intraseasonal variability of the North Brazil Undercurrent forced by remote winds. Journal of Geophysical Research 117, C11024.

- Xu, J., 2003. Sediment flux into the sea as influenced by the changing human activities and precipitation: Example of the Huanghe River, China. Acta Oceanol Sininca 25:125–135.

- Yang S. L., Zhao Q. Y., Belkin IM, 2002. Temporal variation in the sediment load of the Yangtze River and the influences of human activities. J Hydrol 263:56–71.

- Wang, Y., 2004. Ocean Tide Modeling in the Southern Ocean. Technical Report 471. Department of Civil and Environmental Engineering and Geodetic Science. The Ohio State University, Columbus, Ohio.

- Wei, X., Schramkowski, G. P., & Schuttelaars, H. M. (2016). Salt dynamics in well-mixed estuaries: Importance of advection by tides.Journalof Physical Oceanography,46, 1457–1475. https://doi.org/10.1175/JPO-D-15-0045.1.

- Wells, A. W., and J. R. Young, 1992. Long-term variability and predictability of Hudson River physical and chemical characteristics, inEstuarineResearch in the 1980s, edited by C. Lavett Smith, pp. 29–58, S.U.N.Y.Press, Albany, N. Y.

- Wilson, W. D., Johns, W. E., and Garzoli, S. L.: Velocity structure of North Brazil Current rings, Geophys. Res. Lett., 29(8), 1273, doi:10.1029/2001GL013869, 2002.

- Wright, L.D., Coleman, J.M., 1973. Variations in morphology of major river deltas as functions of ocean wave and river discharge regimes. Am. Assoc. Pet. Geol. Bull.370–398.

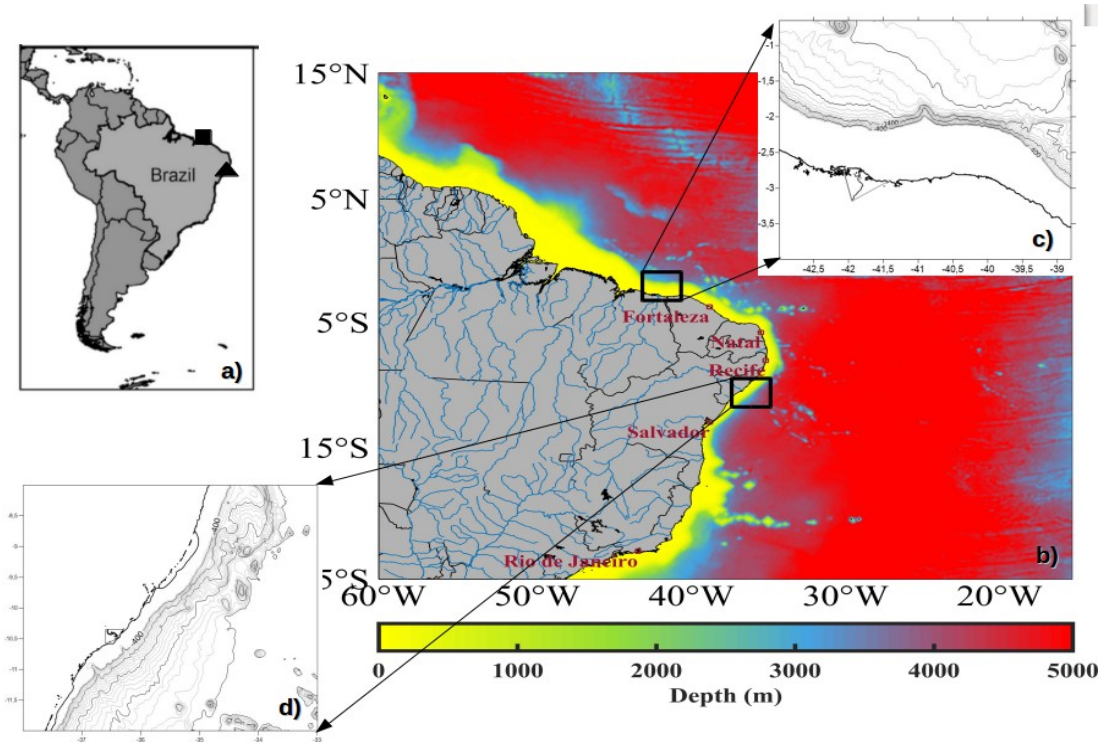

Figure 1: Location of Brazil in South-America, and of the Parnaiba and Sao Francisco estuaries in the northeastern region ('a' adapted from [Aquino da Silva et al., 2019]). 'b' shows the geographic extension of the domain of the 'Tidal' simulation at 1/12º with 50 levels, where the boxes highlight the two embedded zooms of the Parnaiba and Sao Francisco deltas and adjacent platforms (respectively 'c' and 'd)', realized using [GEBCO, 2003] and [Gorelick et al., 2017]).

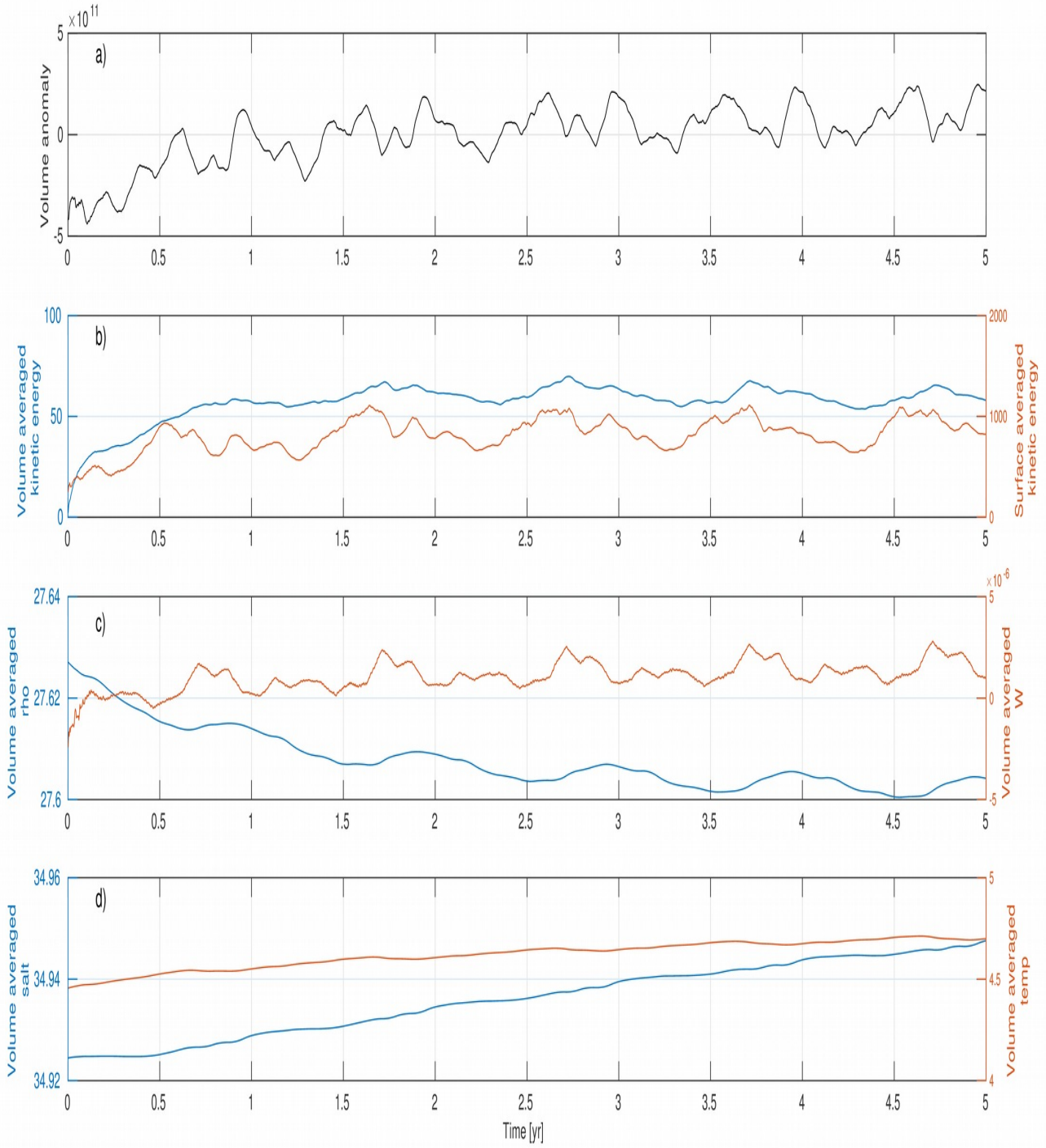

Figure 2: Temporal series of different surface and volume averaged variables ('a' volume anomaly [km³], 'b' kinetc energy [cm²/s²], 'c' density [kg/m³] on the left y-axis and vertical velocity [m/s] on the right y-axis, 'd' salt [PSU] on the left y-axis and temperature [°C] on the right y-axis) of the simulation at 1/12º with 50 levels, whose first 18 months can be considered a spin-up period.

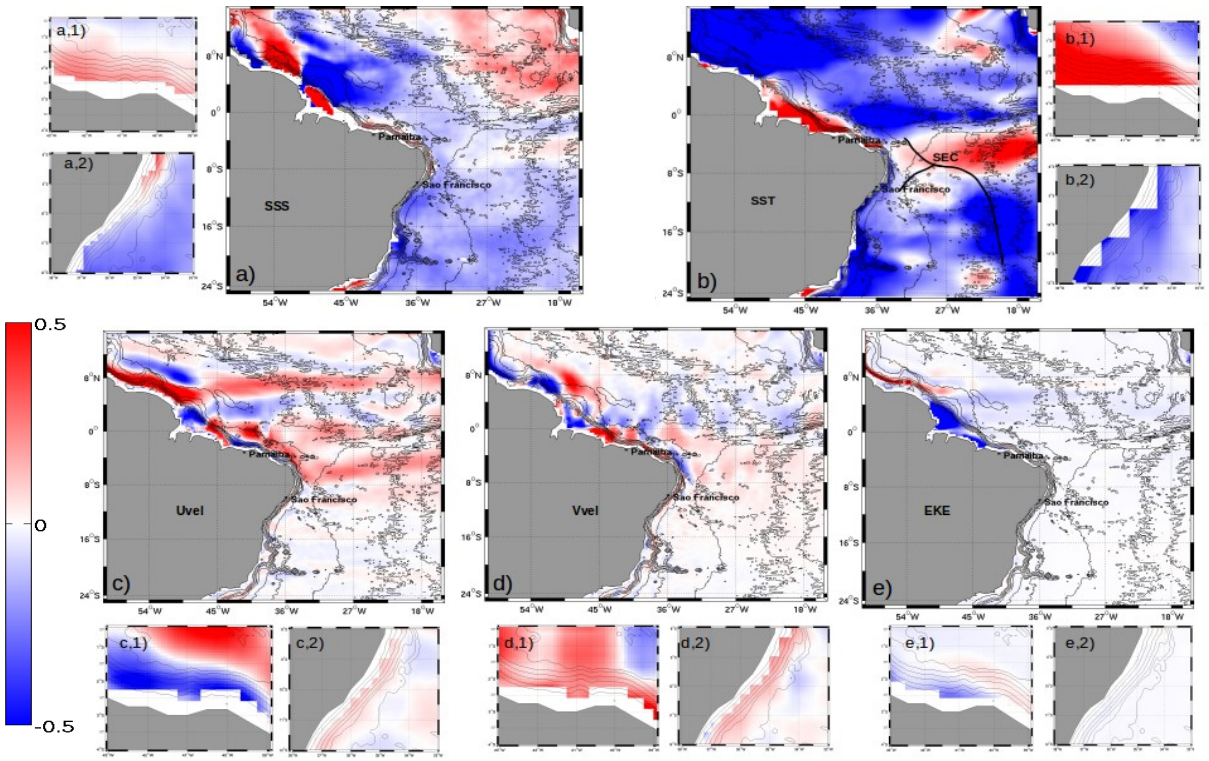

Figure 3: Difference maps of Sea Surface Salinity (a), Sea Surface T emperature (b), zonal U (c) and meridional V (d) velocities, Eddy Kinetic Enenrgy (e) between the monthly means of the 'Tidal' run and satellite-observations interpolated in the model grid.With '1' and '2' are indicated the Parnaiba and Sao Francisco zooms for each of these variables, while in subplot ' b' the South-Equatorial Current (SEC) bifurcation has been sketched following Rodrigues et al. [2007].

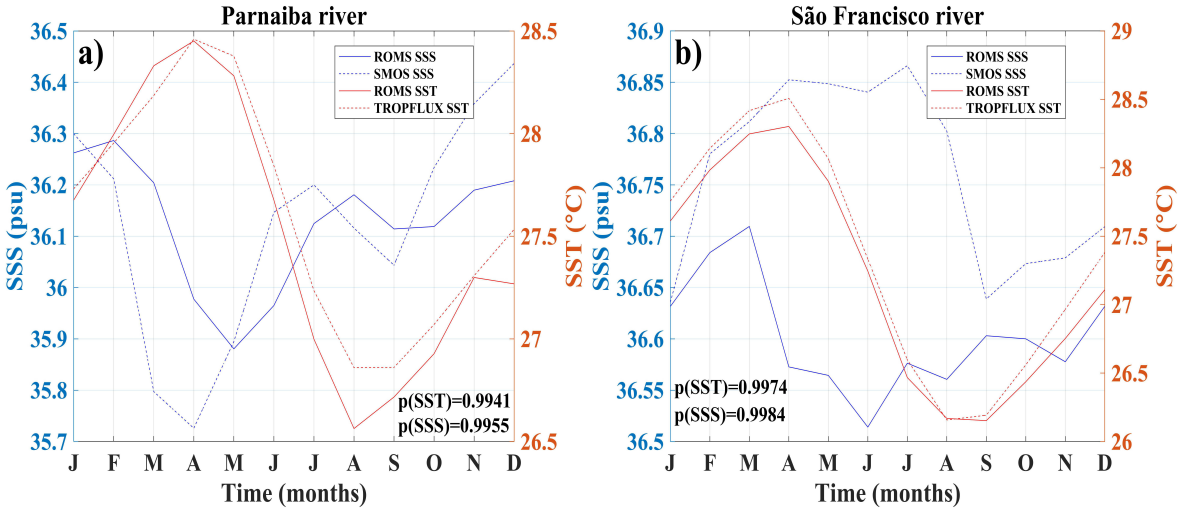

Figure 4: Monthly timeseries of SST (red curves) and SSS (blue curves) comparing the seasonal cycles of the ROMS output (average files from the last 8 years of the Tidal simulation) and the satellite observations used for the model validatio(TropFlux and SMOS datasets, respectively) within the nested domains of the Parnaiba (a) and the Sao Francisco (b) estuaries. The 'p' values at the bottom of each graph represent the significance coefficients from the 't-student' test used to statistically corroborate the robustness of the comparison results.

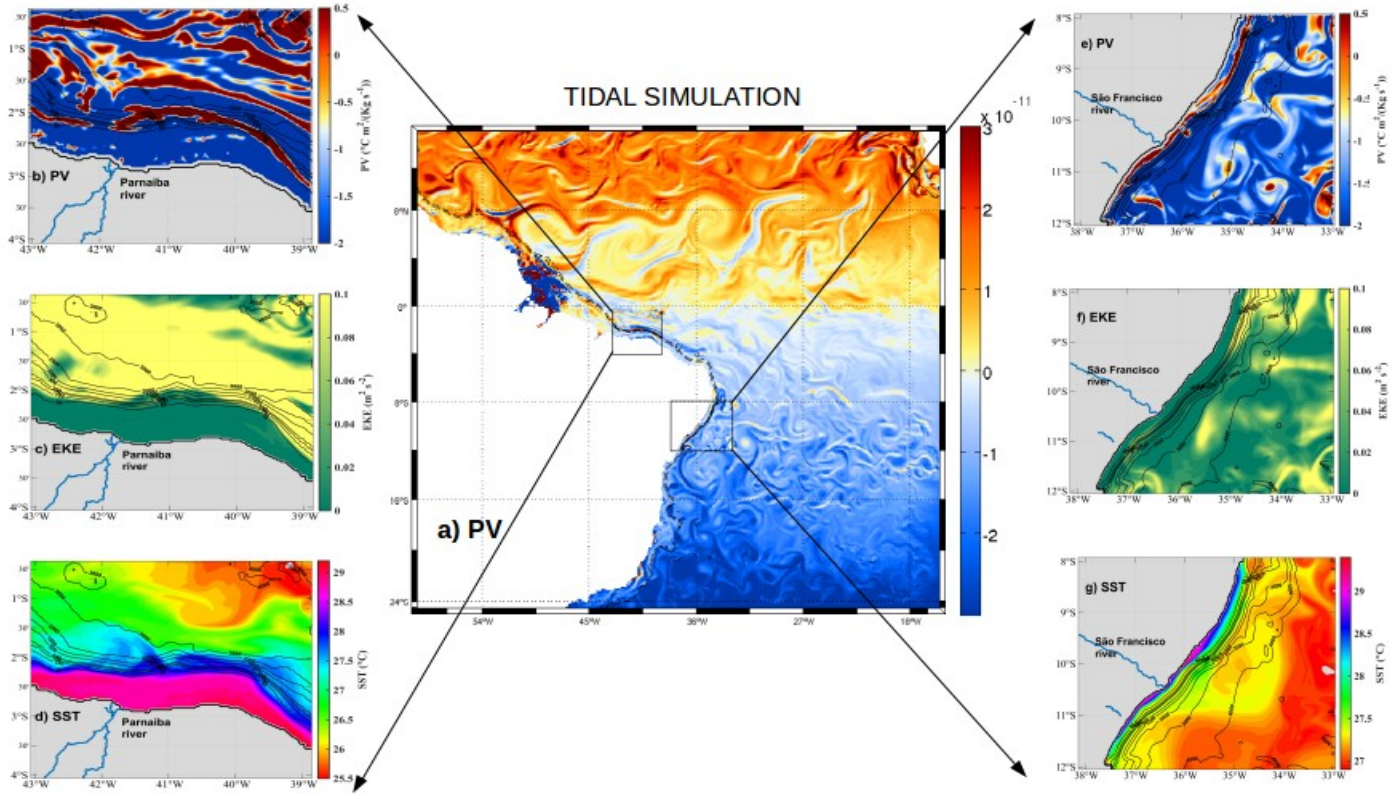

Figure 5: Instantaneous surface maps of Potential Vorticity for the parent grid (a) and the Parnaiba and Sao Francisco child grids (b and e), as well as estimates of EKE (c and f) and SST (d and g) from the 'Tidal' simulation. In 'a' the Abrolhos Bank and the Vitoria-Trindade Ridge are marked by respectively a black asterisk and a black square.

Figure 6: Same as Figure 5 for the 'No- tide' simulation.

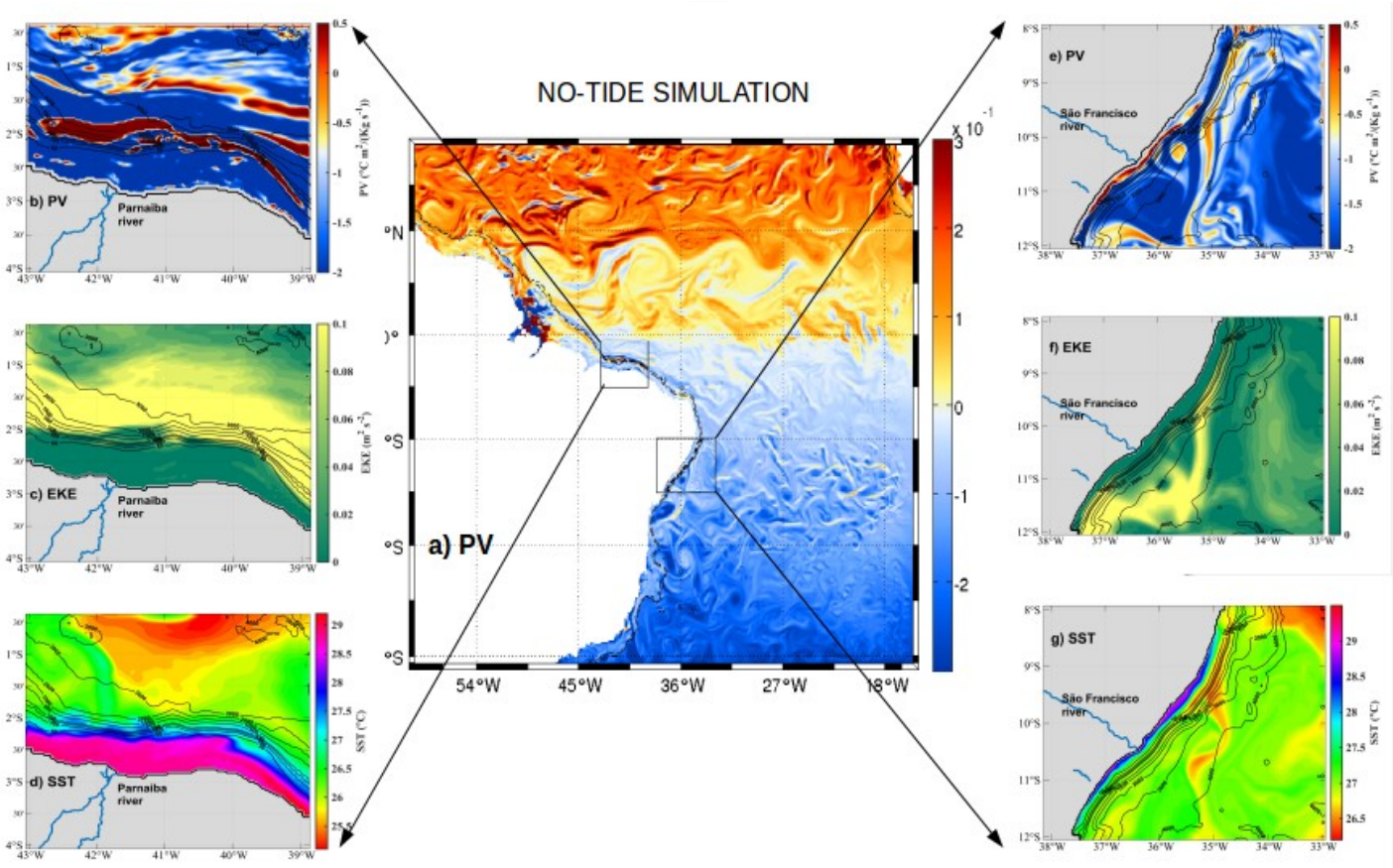

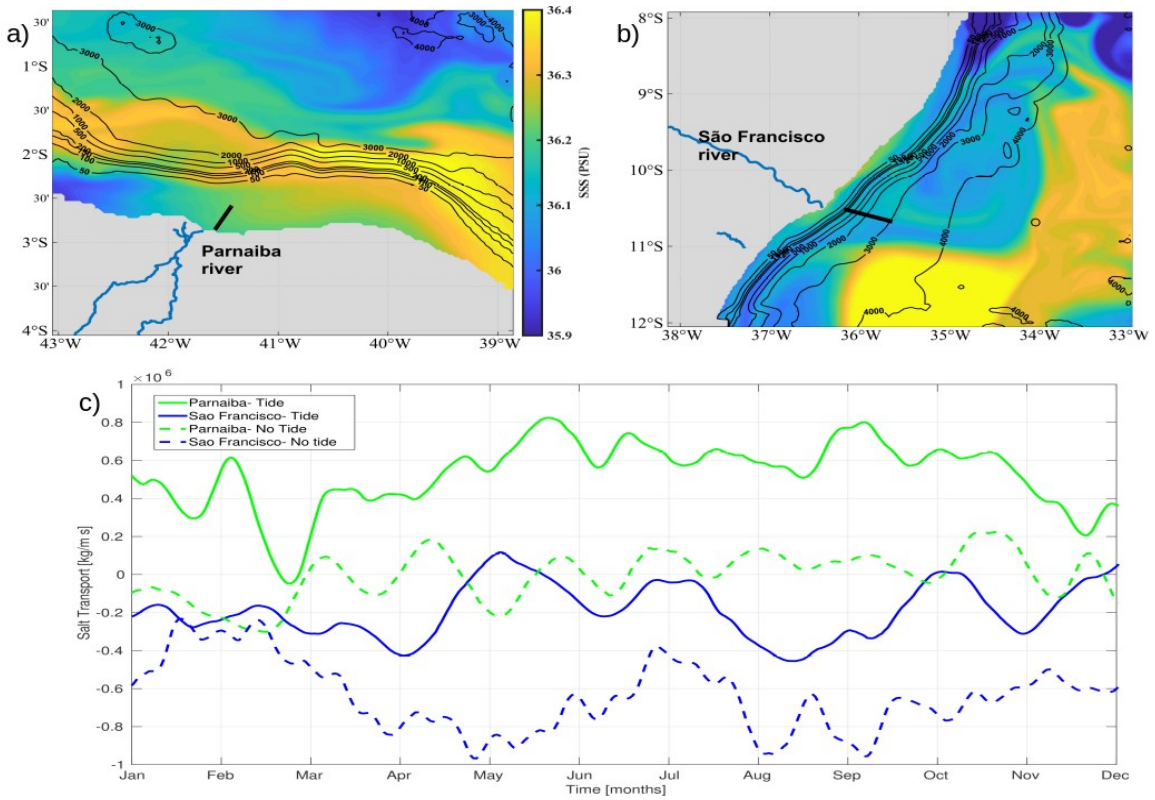

Figura 7: Sea Surface Salinity mean maps from the model last year (Y10) of the 'Tidal' simulation for the Parnaiba and the Sao Francisco zooms (respctevely 'a' and 'b'), showing the location of the transects across the continental platform along which the times series of the daily averages of salt transports ('c') were calculated for the 'Tidal' and 'No-tide' runs.

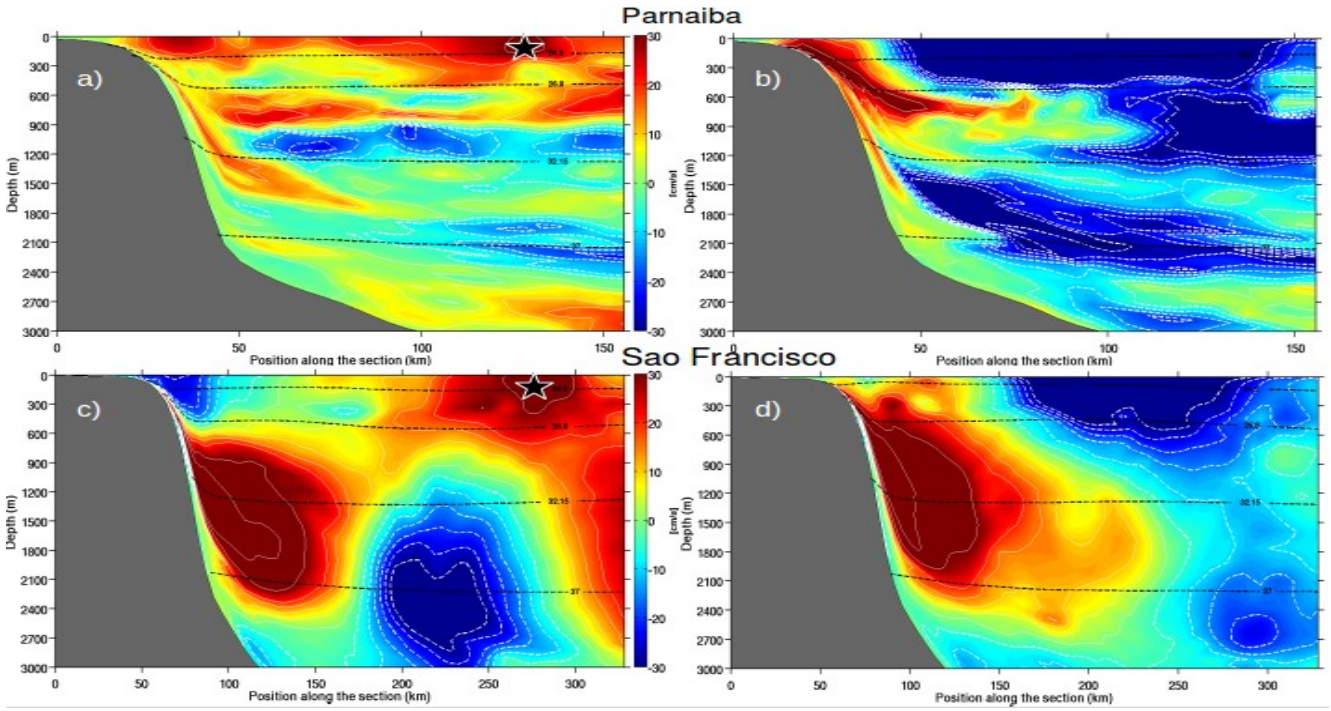

Figure 8: Vertical sections of instantaneous meridional (left) and zonal (right) velocities along the transects shown in Figures 7 a-b for the Parnaiba ('a', 'b') and the Sao Francisco ('c' ,'d') child grids. Positive (negative) values indicated by solid (dashed) white lines correspond to northward (southward) current, black dashed lines identify isopycnals' position along the water column.The black stars in 'a' and 'c' mark the stations where the profiles of Figure 9 were traced.

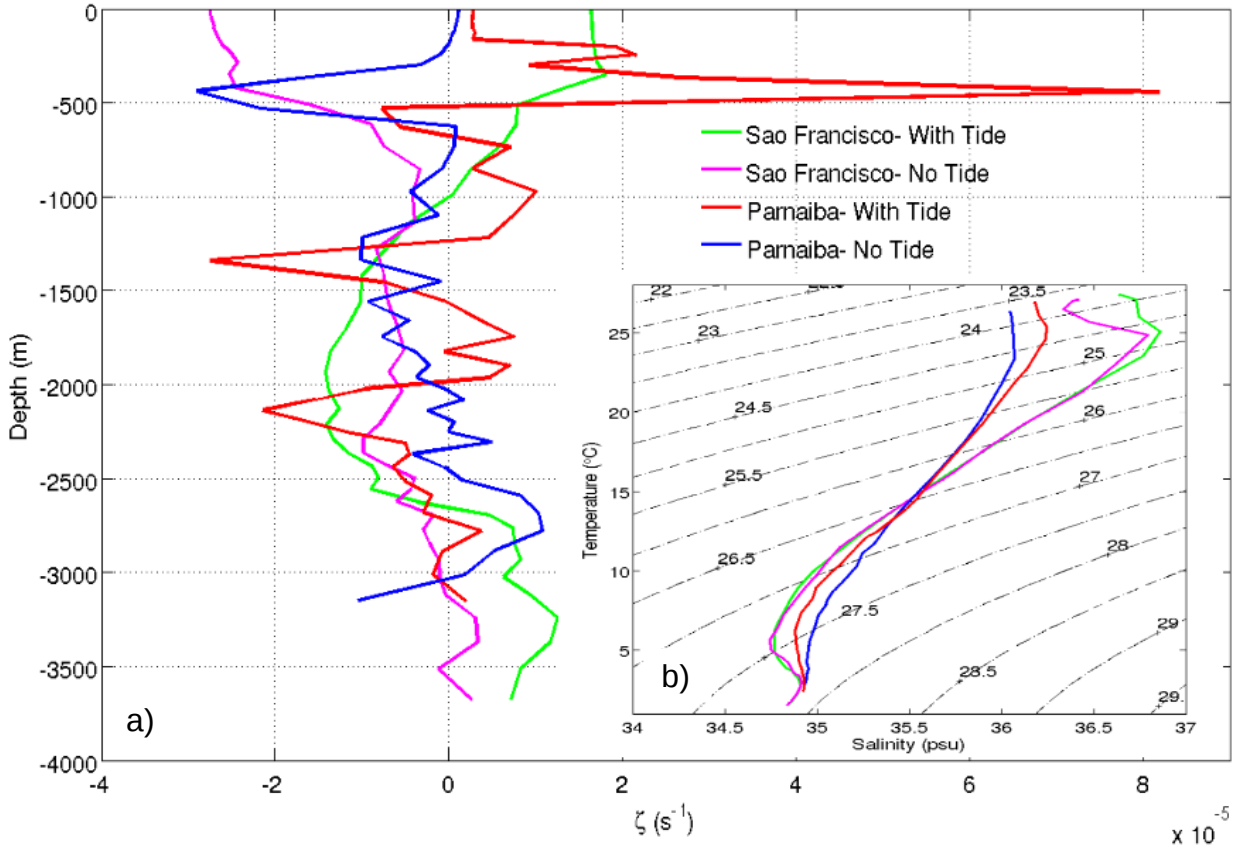

Figure 9: Instantaneous profiles of Relative Vorticity ('a') traced at the locations indicated by black stars in the sections of Figures 7a-c, for the 'Tidal' and 'No-tide' configurations and for both the child grids of the Parnaiba and Sao Francisco deltas; in 'b' the correspondant Temperature-Salinity diagrams plotted at the same stations.

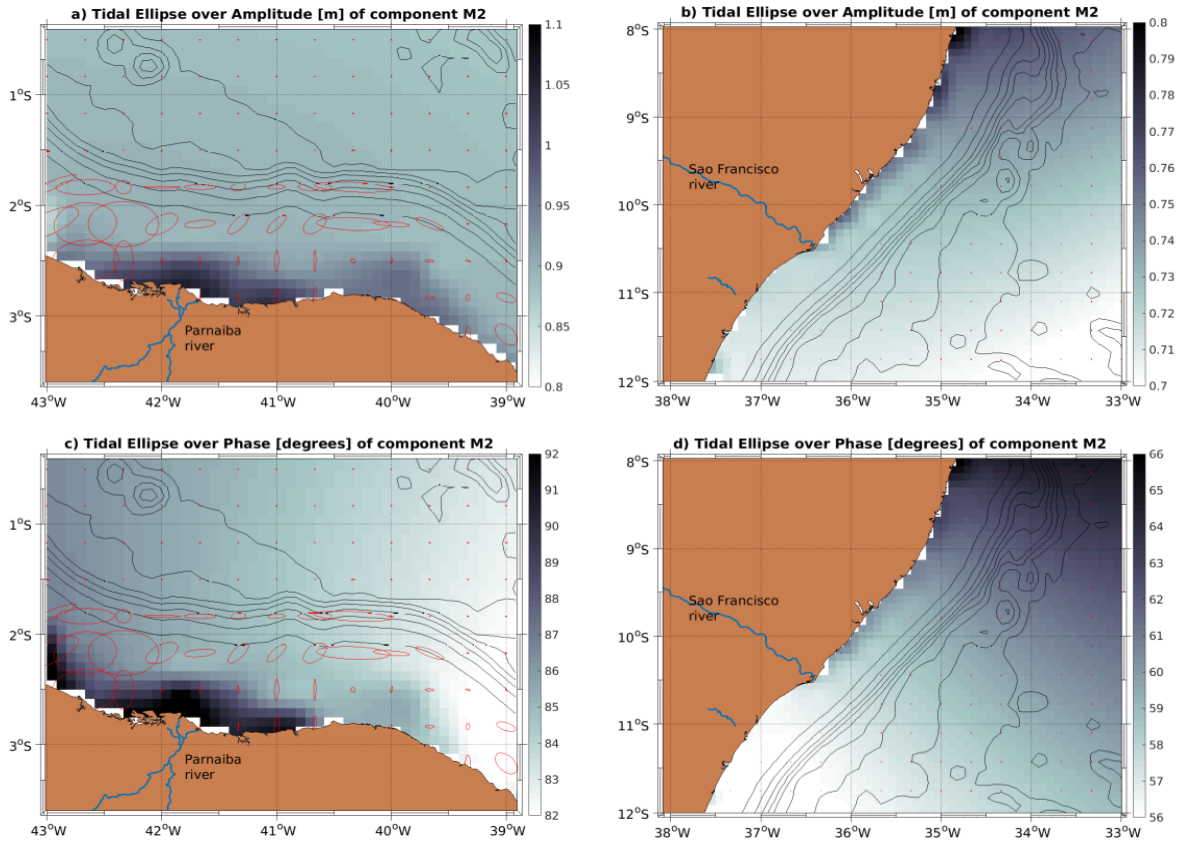

Figure 10: M2 Tidal ellipses (red line) plotted over surface maps of the amplitude and phase of this tidal component for the Parnaiba (respectively 'a' and 'c') and Sao Francisco nested domains ('b' and 'd').

Author declaration

1. Conflict of Interest

☐ Potential conflict of interest exists:

We wish to draw the attention of the Editor to the following facts, which may be considered as potential conflicts of interest, and to significant financial contributions to this work:

The nature of potential conflict of interest is described below:

☒ No conflict of interest exists.

We wish to confirm that there are no known conflicts of interest associated with this publication and there has been no significant financial support for this work that could have influenced its outcome.

2. Funding

☒ Funding was received for this work.

All of the sources of funding for the work described in this publication are acknowledged below:

The CAPES PNPD Brazilian scholarship (Portaria 086/2013) for having supported the author's research as postdoctorate-fellow at UFPE.

☐ No funding was received for this work.

3. Intellectual Property

☒ We confirm that we have given due consideration to the protection of intellectual property associated with this work and that there are no impediments to publication, including the timing of publication, with respect to intellectual property. In so doing we confirm that we have followed the regulations of our institutions concerning intellectual property.

4. Research Ethics

☐ We further confirm that any aspect of the work covered in this manuscript that has involved human patients has been conducted with the ethical approval of all relevant

bodies and that such approvals are acknowledged within the manuscript.

☐ IRB approval was obtained (required for studies and series of 3 or more cases)

☐ Written consent to publish potentially identifying information, such as details or the case and photographs, was obtained from the patient(s) or their legal guardian(s).

5. Authorship

The International Committee of Medical Journal Editors (ICMJE) recommends that authorship be based on the following four criteria:

1. Substantial contributions to the conception or design of the work; or the acquisition, analysis, or interpretation of data for the work; AND
2. Drafting the work or revising it critically for important intellectual content; AND
3. Final approval of the version to be published; AND
4. Agreement to be accountable for all aspects of the work in ensuring that questions related to the accuracy or integrity of any part of the work are appropriately investigated and resolved.

All those designated as authors should meet all four criteria for authorship, and all who meet the four criteria should be identified as authors. For more information on authorship, please see http://www.icmje.org/recommendations/browse/roles-and-responsibilities/defining-the-role-of-authors-and-contributors.html#two.

☒ All listed authors meet the ICMJE criteria. We attest that all authors contributed significantly to the creation of this manuscript, each having fulfilled criteria as established by the ICMJE.

☐ One or more listed authors do(es) not meet the ICMJE criteria.

We believe these individuals should be listed as authors because:

☒ We confirm that the manuscript has been read and approved by all named authors.

☐ We confirm that the order of authors listed in the manuscript has been approved by all named authors.

6. Contact with the Editorial Office

The Corresponding Author declared on the title page of the manuscript is:

Tonia Astrid Capuano

☒This author submitted this manuscript using his/her account in EVISE.

☒We understand that this Corresponding Author is the sole contact for the Editorial process (including EVISE and direct communications with the office). He/she is responsible for communicating with the other authors about progress, submissions of revisions and final approval of proofs.

☐We confirm that the email address shown below is accessible by the Corresponding Author, is the address to which Corresponding Author's EVISE account is linked, and has been configured to accept email from the editorial office of American Journal of Ophthalmology Case Reports:

☐Someone other than the Corresponding Author declared above submitted this manuscript from his/her account in EVISE:

☐We understand that this author is the sole contact for the Editorial process (including EVISE and direct communications with the office). He/she is responsible for communicating with the other authors, including the Corresponding Author, about progress, submissions of revisions and final approval of proofs.

I the undersigned agree with all of the above.

Author's name (Fist, Last)	Signature	Date
1. Tonia Astrid Capuano		10/11/2020

Declaration of interests

☒ The authors declare that they have no known competing financial interests or personal relationships that could have appeared to influence the work reported in this paper.

☐ The authors declare the following financial interests/personal relationships which may be considered as potential competing interests:

Recife, 30th of April 2020